Article

SOURCE DATA | TRANSPARENT PROCESS

THE EMBO JOURNAL

Fam60a defines a variant Sin3a-Hdac complex in embryonic stem cells required for self-renewal

Gundula Streubel[1], Darren J Fitzpatrick[1], Giorgio Oliviero[2], Andrea Scelfo[3], Bruce Moran[2], Sudipto Das[4], Nayla Munawar[2], Ariane Watson[2], Kieran Wynne[2], Gian Luca Negri[5], Eugene T Dillon[2], SriGanesh Jammula[3], Karsten Hokamp[1], Darran P O'Connor[4], Diego Pasini[3], Gerard Cagney[2,†] & Adrian P Bracken[1,*,†]

Abstract

Sin3a is the central scaffold protein of the prototypical Hdac1/2 chromatin repressor complex, crucially required during early embryonic development for the growth of pluripotent cells of the inner cell mass. Here, we compare the composition of the Sin3a-Hdac complex between pluripotent embryonic stem (ES) and differentiated cells by establishing a method that couples two independent endogenous immunoprecipitations with quantitative mass spectrometry. We define the precise composition of the Sin3a complex in multiple cell types and identify the Fam60a subunit as a key defining feature of a variant Sin3a complex present in ES cells, which also contains Ogt and Tet1. Fam60a binds on H3K4me3-positive promoters in ES cells, together with Ogt, Tet1 and Sin3a, and is essential to maintain the complex on chromatin. Finally, we show that depletion of Fam60a phenocopies the loss of Sin3a, leading to reduced proliferation, an extended G1-phase and the deregulation of lineage genes. Taken together, Fam60a is an essential core subunit of a variant Sin3a complex in ES cells that is required to promote rapid proliferation and prevent unscheduled differentiation.

Keywords embryonic stem cell; Fam60a; self-renewal; Sin3a-Hdac complex
Subject Categories Chromatin, Epigenetics, Genomics & Functional Genomics; Stem Cells; Transcription
DOI 10.15252/embj.201696307 | Received 16 December 2016 | Revised 18 April 2017 | Accepted 22 April 2017 | Published online 29 May 2017
The EMBO Journal (2017) 36: 2216–2232

See also: **R Pantier *et al*** (August 2017)

Introduction

The chromatin of embryonic stem (ES) cells is characterized by unique features ensuring their responsiveness to differentiation cues (Liang & Zhang, 2013; Allis & Jenuwein, 2016). When induced to differentiate, ES cells lose their proliferative capacity, concomitant with dynamic changes in the profiles of histone post-translational modifications (PTMs) and the formation of a more closed chromatin state (Chen & Dent, 2014; Di Giammartino & Apostolou, 2016; Ruijtenberg & van den Heuvel, 2016). Consistent with the open and accessible chromatin state of ES cells, histone acetylation is more abundant in pluripotent compared to differentiated cells (Lee *et al*, 2004; Meshorer & Misteli, 2006; Meshorer *et al*, 2006; Efroni *et al*, 2008). The levels and profiles of histone acetylation are regulated by class I histone deacetylase (Hdacs) enzymes that typically assemble into large multi-protein chromatin complexes together with several other chromatin-associated proteins (Ho & Crabtree, 2010; Kelly & Cowley, 2013). The three best characterized Hdac1/2 containing complexes, Sin3-Hdac, NuRD and CoREST, are essential during early embryonic development and also in adult tissue maintenance (McDonel *et al*, 2009; Kelly & Cowley, 2013). While these Hdac complexes were first identified as being transcriptional repressors, recent studies have revealed that they also have roles associated with gene activation (van Oevelen *et al*, 2010; Reynolds *et al*, 2013; Baymaz *et al*, 2015). These roles are thought to include fine-tuning of ongoing transcription and "priming" gene promoters for subsequent transcriptional responses (Reynolds *et al*, 2013; Laugesen & Helin, 2014). However, due to the modular assemblies of these large multi-protein complexes, it has so far proved challenging to link particular complex subunits with specific cell lineages or to specific biological functions (Baymaz *et al*, 2015).

In mammals, the prototypical Sin3a-Hdac complex either contains the Sin3a or Sin3b protein. These homologous proteins form different complexes and fulfil non-redundant biological

1 Smurfit Institute of Genetics, Trinity College Dublin, Dublin 2, Ireland
2 School of Biomolecular and Biomedical Science, University College Dublin, Dublin 4, Ireland
3 Department of Experimental Oncology, European Institute of Oncology, Milan, Italy
4 Department of Molecular and Cellular Therapeutics, Royal College of Surgeons in Ireland, Dublin 2, Ireland
5 Department of Molecular Oncology, British Columbia Cancer Research Center, Vancouver, BC, Canada
*Corresponding author. Tel: +353 1 896 4121; E-mail: adrian.bracken@tcd.ie
†These authors contributed equally to this work

functions (Laugesen & Helin, 2014). Importantly, while Sin3b is dispensable for early development in mice, Sin3a is required at the implantation stage when the pluripotent cells of the epiblast undergo their first cell fate transitions (Cowley *et al*, 2005; McDonel *et al*, 2012) and has been recently reported to promote pluripotency in ES cells and iPSC reprogramming (Saunders *et al*, 2017). Moreover, in mice, Sin3a contributes to male germ cell development (Pellegrino *et al*, 2012), myogenesis (van Oevelen *et al*, 2010) as well as T-cell and epidermal tissue homeostasis (Dannenberg *et al*, 2005; Nascimento *et al*, 2011). While the precise composition of Sin3a complexes in different cell types remains unknown, more than a dozen accessory factors have been identified in biochemical purifications performed on cancer cell lines (Grzenda *et al*, 2009). These studies revealed that the Sin3a protein acts as a central scaffold onto which Hdac1/2 and several other proteins assemble. The Sin3a core complex was initially described to contain Hdac1/2, Rbbp4/7, Sud3 which augments Hdac activity, as well as the Sin3-associated proteins (SAPs) Sap18 and Sap30, which bridge interactions within the complex (Hassig *et al*, 1997; Zhang *et al*, 1997, 1998; Laherty *et al*, 1998; Alland *et al*, 2002). Several additional Sin3a accessory proteins have been identified, including Sap25, Sap130, Arid4b (Sap180), Arid4a (Rbp1, Rb-binding protein), Brms1 and Brms1l (breast cancer metastasis suppressor 1), Ing1/2 (Inhibitor of Growth 1/2), Fam60a (Family with Sequence similarity 60 A), Tet1 (Ten-eleven translocation 1) and Ogt (O-GlcNAc transferase; Lai *et al*, 2001; Kuzmichev *et al*, 2002; Yang *et al*, 2002; Fleischer *et al*, 2003; Nikolaev *et al*, 2004; Smith *et al*, 2010, 2012; Williams *et al*, 2011; McDonel *et al*, 2012; Munoz *et al*, 2012). The Sin3a complex has also been reported to associate with several sequence-specific DNA-binding transcription factors with well-established roles in cell cycle control and development, including Rest, Rb, Hbp1, the Myc-inhibitors Mxi1 and Mad1, Klf proteins, Foxk1/2 as well as with the nuclear hormone repressors, N-CoR and SMRT (Silverstein & Ekwall, 2005). However, it is unclear how or whether these DNA-binding transcription factors functionally interplay with the Sin3A complex on a genomewide level. Furthermore, the molecular functions of many of the several more abundant accessory proteins within the Sin3a complex are also unknown. In contrast to the very well-characterized BAF chromatin remodelling and Polycomb complexes, the exact molecular composition of the Sin3a-Hdac complex in different non-cancer cell types has not yet been defined (Lessard *et al*, 2007; Ho *et al*, 2009; Oliviero *et al*, 2016). An unanswered question is whether the numerous accessory proteins reported to interact with Sin3a are part of tissue-specific variants of the Sin3a complex that potentially confer different functions in different lineage types.

To characterize the endogenous composition of the Sin3a complex in ES and differentiated cell types, we established a method to couple two independent endogenous immunoprecipitations with quantitative mass spectrometry. This allowed us to explore the detailed stoichiometry of the Sin3a complex in ES cells before and after differentiation to embryoid bodies (EB) as well as in fibroblasts. We find that the composition of the Sin3a complex changes during ES cell differentiation and identified Fam60a as a key protein that defines a variant complex in ES cells. We show that Fam60a is highly expressed in pluripotent ES cells and its gene locus is bound by E2f1, Nanog and Oct4 (Pou5f1). In ES cells, the Fam60a protein co-binds together with Sin3a and two other ES cell-specific Sin3a complex proteins, Ogt and Tet1, on H3K4me3-positive promoters. Fam60a promotes the stability of Sin3a and its presence on chromatin and, like Sin3a, is crucial for maintaining the potential of ES cells to proliferate rapidly, while ensuring a short G1-phase of the cell cycle, thereby preventing premature lineage priming. These results have important implications for our understanding of the nature and function of multi-protein Hdac1/2 complexes and provide new insights into the link between their dynamic composition changes and the regulation of pluripotency and cell fate decisions.

Results

Fam60a defines a variant Sin3a-Hdac complex present in ES cells

In order to determine the precise composition of the Sin3a-complex in mouse ES cells compared to embryoid bodies (EB) and fibroblasts, we established a strategy to perform endogenous immunoprecipitations coupled with quantitative mass spectrometry (Fig 1A). Immunoprecipitates from three replicates of two different Sin3a antibodies were subjected to label-free mass spectrometry analysis, and the peptides were analysed using MaxQuant (Cox & Mann, 2008). To determine the relative stoichiometries, the relative iBAQ values (Smits *et al*, 2013) were

Figure 1. Endogenous compositional analysis reveals Fam60a defines the Sin3a complex in ES but not in differentiated cells.

A Experimental outline for label-free quantitative mass spectrometry of the Sin3a-Hdac complex in mouse pluripotent and differentiated cells. Immunoprecipitations (IPs) were performed in triplicates on nuclear lysates from embryonic stem (ES) cells, embryoid bodies (EB) and fibroblasts (F) using two Sin3a-specific antibodies (Sin3a antibody 1 from Abcam; Sin3a antibody 2 from Santa Cruz) and IgG as a negative control. The precipitated proteins were subjected to LC-MS/MS following tryptic digestion. The data were analysed using the programs MaxQuant and Perseus.

B Stoichiometric analysis of the composition of the Sin3a complex in ES cells, embryoid bodies (EB) and fibroblasts (F). The scatter plots represent the average iBAQ values (n = 3) relative to the bait protein Sin3a (red). Previously identified members of the Sin3a complex are labelled in green. The Sin3a-associated proteins specifically enriched in ES cells are depicted in blue, those enriched in differentiated lineages in orange.

C The graphs show the relative stoichiometries and standard deviations (SD) of the two independent Sin3a IPs (each performed with three technical replicates) for proteins enriched in ES (blue) or differentiated cells (orange) as well as proteins exemplary for being detected at similar levels in all cell types (green). Only proteins with an iBAQ of at least 0.01 in any of the cell lines are shown.

D Western blot analysis of Sin3a immunoprecipitations in mouse ES cells, EBs and fibroblasts, for the indicated antibodies.

E Model depicts the Fam60a-Sin3a complex composition present in ES cells. Proteins enriched in ES cells are highlighted in blue. Other proteins associated with Sin3a in ES cells are indicated in green. The Fam60a-Sin3a core complex in ES cells containing Sin3a, Sap30, Fam60a, Hdac1 and Rbbp4/7 is presented. The proteins separated by arrows indicate low stoichiometries.

Source data are available online for this figure.

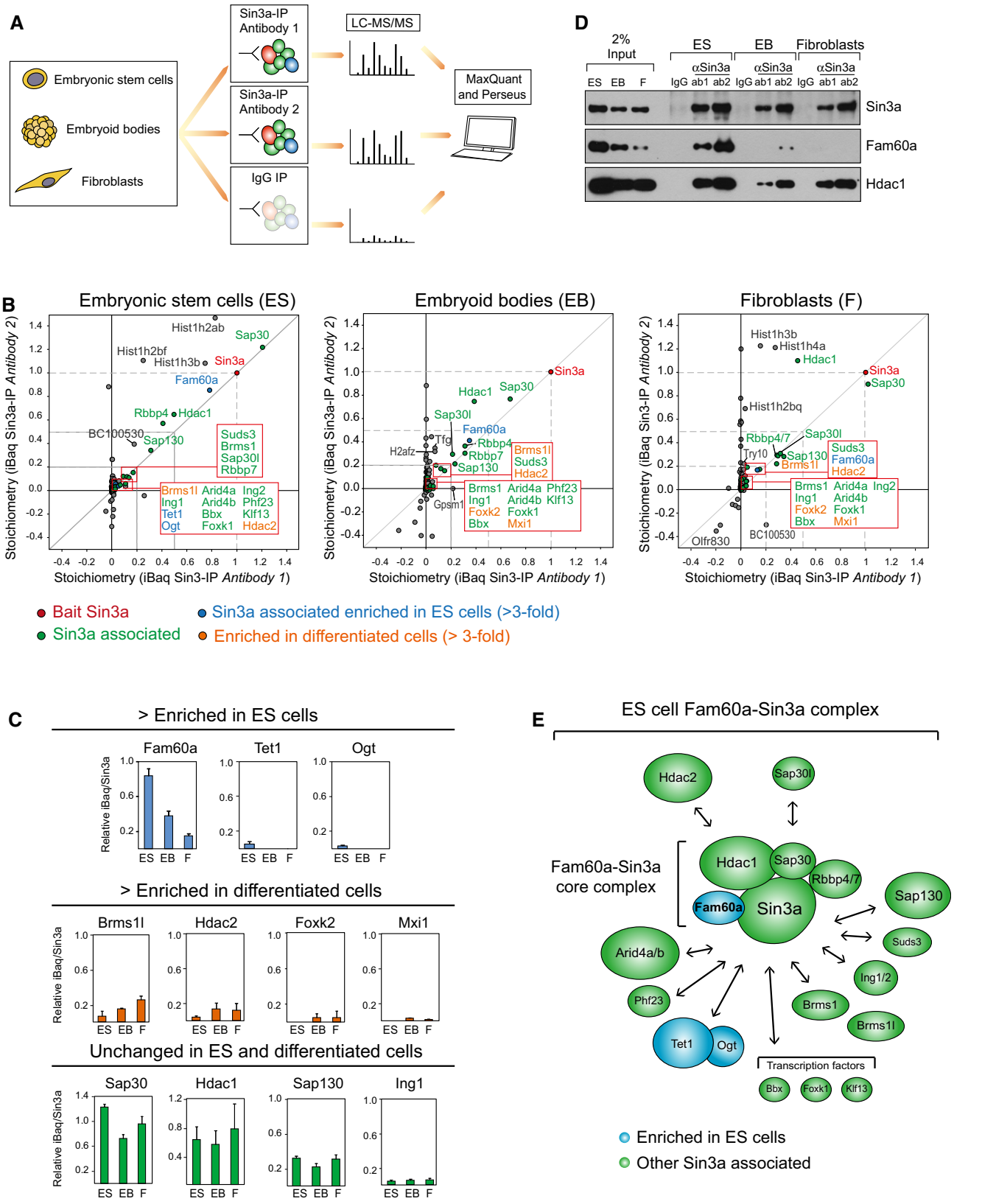

Figure 1.

calculated and represented both as scatter plots (Fig 1B) and in table form (Fig EV1A). While most of the strongest enriched proteins in both Sin3a immunoprecipitations were previously reported to be Sin3a-interacting proteins, several novel proteins were also detected, including Dpy30 (histone methyltransferase complex regulatory subunit), Psme3 (proteasome activator complex subunit 3) and Nono (Non-Pou domain containing octamer-binding protein; Table EV1). Importantly, all of the previously reported members of the Sin3a complex, except Sap18 and Sap25, were found to be significantly immunoprecipitated (*t*-test, FDR 0.01), and several were constitutively present in all three cell types, for example Sap30, Sap130 and Hdac1 and Ing1 (Fig EV1A and Table EV1). Intriguingly, we identified several other proteins that preferentially associate with Sin3a in either ES or in differentiated cells (Figs 1C and EV1A and B). For example, the Fam60a, Tet1 and Ogt proteins were threefold enriched in the Sin3a complex in ES cells, whereas the transcriptional repressors Mxi1 and Foxk2 (Nascimento *et al*, 2011; Bowman *et al*, 2014), as well as the Brms1l and Hdac2 proteins were enriched in differentiated cells (Figs 1C and EV1A). The Fam60a protein was the most striking due to its high relative stoichiometry of nearly 1:1 relative to Sin3a in ES cells, suggesting it is a core member of the Sin3a complex in these cells (Figs 1C and EV1A). In contrast, the Tet1 and Ogt proteins, which were previously reported to interact with the Sin3a complex (Yang *et al*, 2002; Williams *et al*, 2011), while specifically detected in ES cells, had relatively low iBAQ values (Figs 1C and EV1A).

Next, to validate the differential enrichment of Fam60a within the Sin3a complex in ES cells compared to EBs and fibroblasts, we performed Western blot analysis of two independent Sin3a immunoprecipitations and confirmed that, unlike Hdac1, Fam60a is strongly differentially immunoprecipitated from nuclear lysates from ES cells, but not from differentiated cells (Fig 1D). The iBAQ analysis strongly suggests that Fam60a, together with Sin3a, Sap30, Hdac1 and Rbbp4/7, forms the core of a specialized variant Sin3a-Hdac complex, which we refer to as the "Fam60a-Sin3a complex" (Figs 1E and EV1B). Taken together, these data reveal an heretofore unappreciated lineage-specific composition of the Sin3a complex and highlight Fam60a, the defining subunit of the Fam60a-Sin3a complex, as a potential key regulator of the Sin3a complex function in ES cells (Fig 1E).

Fam60a predominantly assembles within the Sin3a complex in ES cells

We next sought to understand the role of Fam60a in ES cells by determining whether it resides only within the Sin3a complex or whether it might also be present in additional chromatin complexes. To address this, we developed a strategy to perform immunoprecipitations of both endogenous and exogenously Flag-tagged Fam60a, coupled with label-free quantitative mass spectrometry (Fig 2A). Western blot analysis of endogenous Fam60a and Flag-Fam60a immunoprecipitations showed that both experiments equivalently precipitated Sin3a and Ogt, but not the negative control, Oct4 (Fig 2B). These immunoprecipitations were then subjected to mass spectrometric analysis, which revealed that Fam60a associates almost exclusively with members of the Sin3a complex (Fig 2C and Table EV2). In fact, of the 20 most strongly associated proteins in both the endogenous and exogenous Fam60a immunoprecipitations, 18 were already previously reported as being Sin3a-interacting proteins (Fig 2D and Table EV2). Of note, the Sin3a association with Foxk2 and Mxi1, which was detected in EBs and fibroblast cells (Fig 1B), was not observed in the Fam60a immunoprecipitations in ES cells (Table EV2), further supporting the idea that they do not associate with the complex in pluripotent cells. Although we cannot rule out that a small proportion of Fam60a proteins have Sin3a-independent interaction partners, our data support a model in which Fam60a is a subunit unique to the Sin3a complex and not present in other chromatin complexes.

The *Fam60a* gene is highly expressed in ES cells and is bound by E2f and pluripotency transcription factors

We next wished to explain the high levels of Fam60a in the Sin3a complex in ES cells and speculated that its protein levels might be down-regulated during differentiation. We monitored the protein levels of Fam60a during differentiation of ES cells to embryoid bodies (EBs) and found it decreased strongly, while the levels of the two other Sin3a complex core components, Sin3a and Hdac1, were less affected (Fig 3A). As expected, the protein levels of the pluripotency factor Oct4 decreased while Cbx8, a protein known to be induced during ES cell differentiation (Pasini *et al*, 2007), increased. In parallel, in NTERA-2 human pluripotent embryonic carcinoma cells induced to differentiate upon RA addition, we observed that the protein levels of human FAM60A protein decreased together with SALL4 and OCT4 in mass spectrometry analysis of chromatin-associated proteins (Appendix Fig S1 and Table EV3), suggesting that the transcriptional regulation of Fam60a in pluripotent cells is conserved between mouse and human. Furthermore, the mRNA levels of *Fam60a*, but not of *Sin3a*, also decreased during ES cell differentiation (Fig 3B), suggesting that it is regulated at the transcriptional level.

To begin to understand how the *Fam60a* gene is transcriptionally regulated in ES cells, we searched several genomewide mapping ChIP-Seq data sets of transcription factors with an established roles in ES cells (GEO Datasets, ENCODE) and identified E2f1, a transcription factor associated with cellular proliferation (Bracken *et al*, 2004), and the core pluripotency transcription factors, Nanog and Oct4, as potential upstream regulators. We next performed chromatin immunoprecipitations (ChIPs) of E2f1, Oct4 and Nanog, at both the promoter and an upstream enhancer of Fam60a gene locus, which we found to be predicted by chromatin capture analysis (Schoenfelder *et al*, 2015). This revealed that E2f1 binds strongly to the Fam60a promoter and the upstream enhancer, while both Oct4 and Nanog bind only to the enhancer (Fig 3C). Next, to determine whether *Fam60a* mRNA levels are dependent on the core pluripotency network, we depleted the levels of Oct4 and observed a significant decrease in the levels of *Fam60a* mRNA (Fig 3D). However, *Fam60a* mRNA levels could be decreasing in this experiment due to the fact that these cells were differentiating and not because the loss of Oct4 was directly mediating transcriptional activation. Taken together, these data establish that Fam60a is a chromatin-associated factor, highly expressed in pluripotent ES cells, and suggest that it is, at least in part, regulated on the transcription level by the E2f and core pluripotency transcription factor networks.

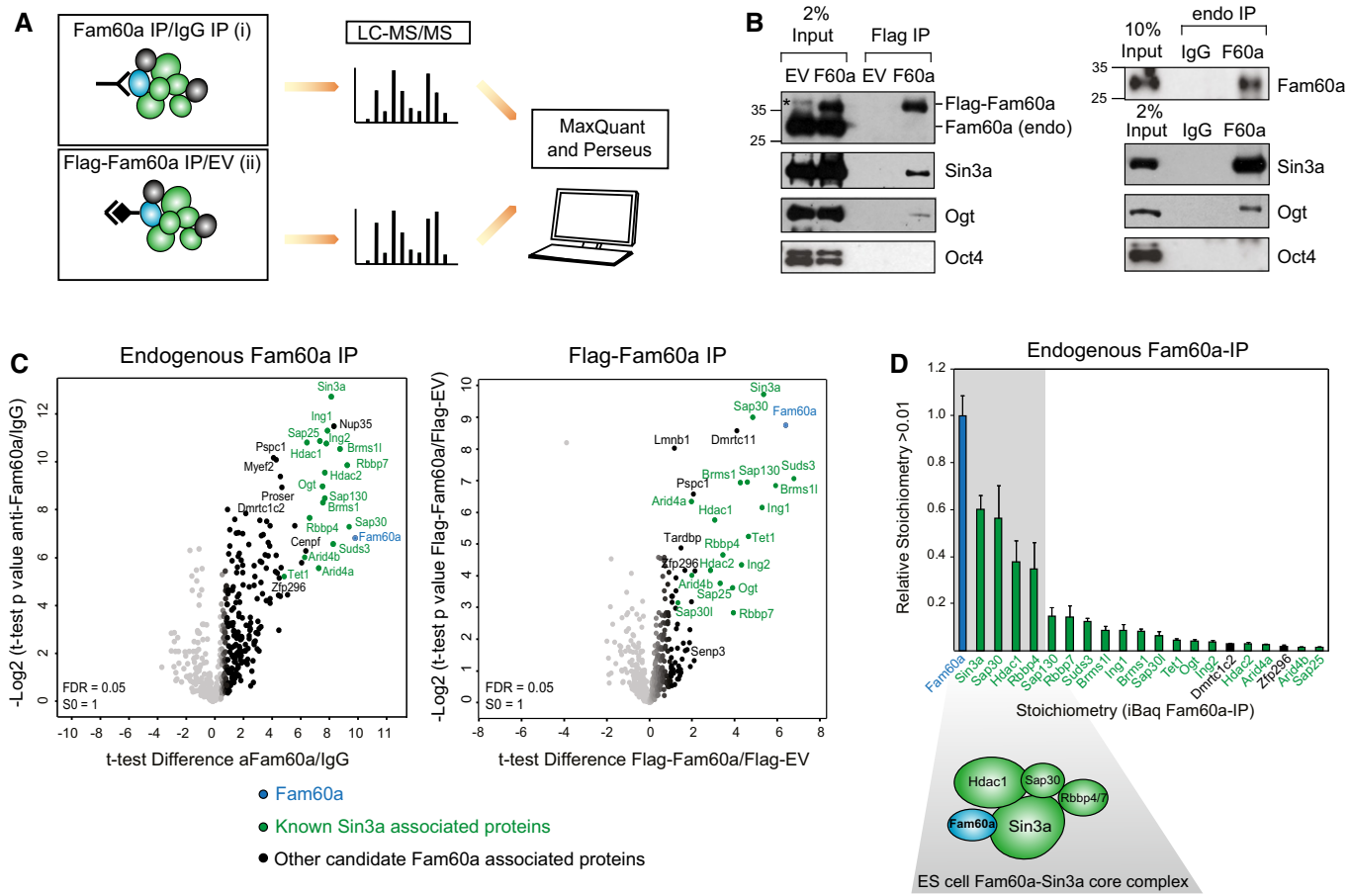

Figure 2. Fam60a resides predominantly within the Sin3a chromatin complex in ES cells.

A Outline of experimental strategy to identify Fam60a-associated proteins in ES cells, using a combination of endogenous and exogenous approach IPs. The IPs were performed using (i) an antibody specific for the endogenous Fam60a protein compared to an IgG antibody as a negative control in biological duplicates and (ii) Flag-IPs from two independent mouse ES cell clones stably expressing Flag-Fam60a compared to empty vector control clones as a negative control. Each IP was performed in technical triplicates. The LC-MS/MS data were analysed with MaxQuant.

B Western blot analysis of exogenous Flag-Fam60a (left panel) and endogenous Fam60a (right panel) immunoprecipitations using the indicated antibodies. Sin3a and Ogt are included as positive controls, while Oct4 is a negative control. * = A background, non-specific band.

C Volcano plots for endogenous Fam60a and exogenous Flag-Fam60a immunoprecipitations. The blue dot indicates the bait Fam60a. Known Sin3a complex members are highlighted in green, while the black dots represent other proteins. The *x*- and *y*-axis values were calculated from six replicates, respectively.

D The graph shows relative stoichiometry enrichments of the top 20 ranked Fam60a-interacting proteins significantly immunoprecipitated by Fam60a antibody and by Flag-Fam60a (Table EV2). The relative stoichiometries of the endogenous Fam60a immunoprecipitations are shown (average relative iBAQ values from six data points). The data means ± SD of six replicates of IgG and Fam60a IPs are presented. Blue represents the bait Fam60a, and green depicts known Sin3a-interacting proteins. Two other proteins, not previously known to interact with Sin3a, are depicted in black. The Fam60a-Sin3a core complex is illustrated below the graph.

Source data are available online for this figure.

Fam60a binds together with Sin3a, Ogt and Tet1 on H3K4me3-positive promoters in ES cells

We next wished to determine the genomewide chromatin binding profile of Fam60a in ES cells compared to Sin3a and the other ES cell-specific Fam60a-Sin3a complex-associated factors, Ogt and Tet1. To do this, we performed ChIP-Seq analysis for Fam60a in mouse ES cells and compared it to previously published genome-wide enrichment profiles of Sin3a, Tet1, Ogt, H3K4me3, polymerase II and H3K27me3 (Fig 4). Strikingly, this revealed that Fam60a binds together with Sin3a, Tet1 and Ogt on the majority of H3K4me3-positive promoters in ES cells (Fig 4A). A quantitative Venn diagram analysis confirmed an almost perfect overlap of Fam60a together with Sin3a, Tet1 and Ogt on H3K4me3- and polymerase II-positive gene promoters (Fig 4B). Interestingly, the majority of Fam60a target sites (81%) and Sin3a (68%) are located at promoter regions, comparable to the polymerase II (76%) profile (Fig 4C). This contrasts with the considerably lower proportion of binding of Ogt (39%) and Tet1 (48%) to promoters. While both Ogt and Tet1 have previously been reported to preferentially co-localize around TSSs of CpG-rich genes, they were also shown to bind to intergenic regions in the genome (Williams *et al*, 2011; Wu & Zhang, 2011; Vella *et al*, 2013), suggesting that they may have roles independent of the Fam60a-Sin3a complex at these non-promoter regions.

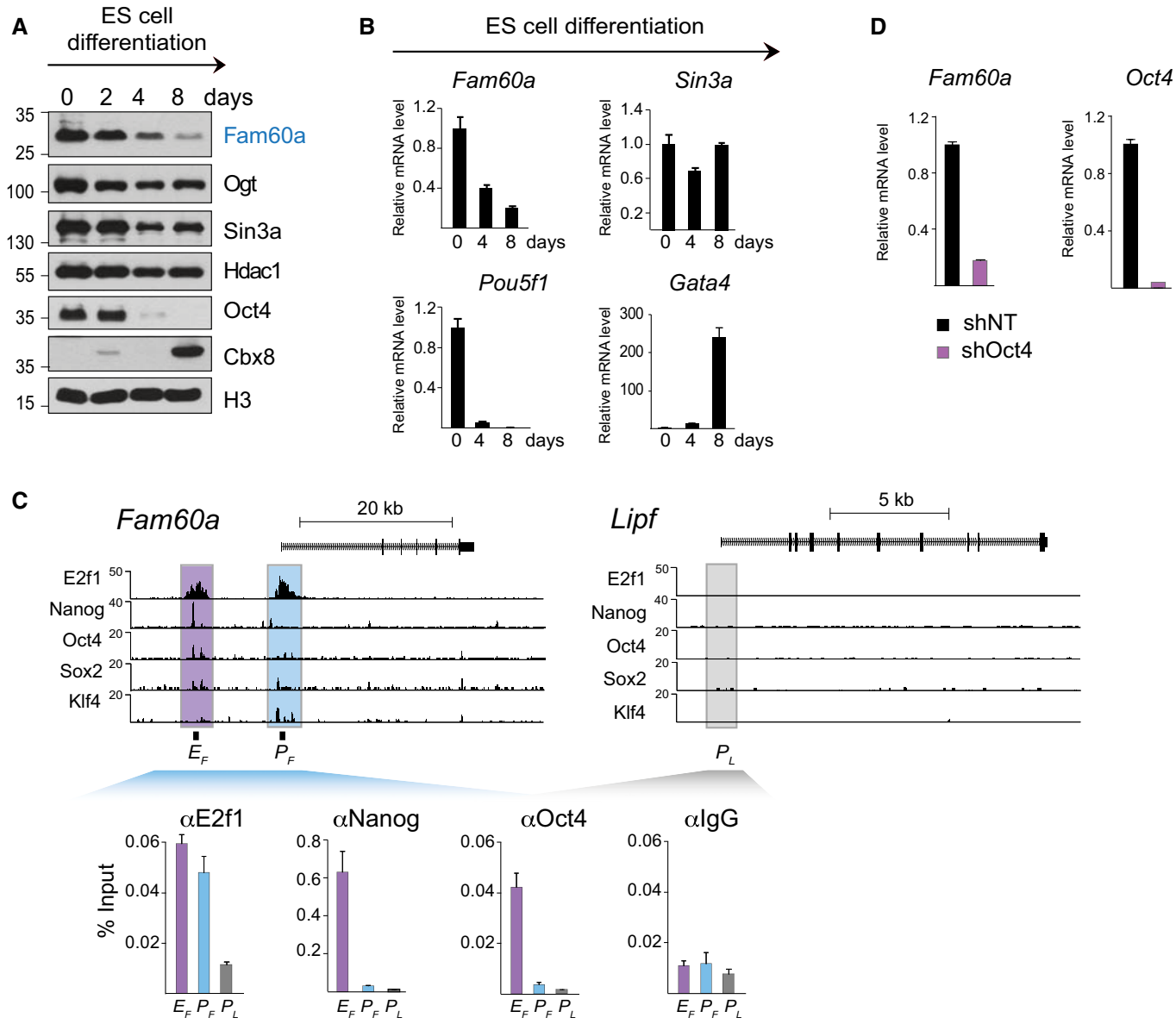

Figure 3. ***Fam60a*** **is an E2f, Oct4 and Nanog target gene highly expressed in proliferating ES cells.**

A Western blots show that the Fam60a protein is down-regulated during differentiation of mouse E14 ES cells. Nuclear lysates were harvested from undifferentiated ES cells and from differentiating ES cells after 2, 4 and 8 days induction to form embryoid bodies. Western blot analysis was performed with the indicated antibodies.

B RT–qPCR analysis of the mRNA levels of *Fam60a*, *Sin3a*, *Oct4* (*Pou5f1*) and the endodermal lineage marker *Gata4* following differentiation of ES cells for 4 and 8 days.

C UCSC genome browser tracks depict the binding of E2f1 and the ES cell transcription factors Nanog, Oct4, Sox2 and Klf4 at the enhancer (E) and promoter (P) region (black bars) of the *Fam60a* gene. The *Lipf* gene promoter is included as negative control. The lower panel represents quantitative ChIP-qPCR analyses of Nanog, Oct4, E2f1 and IgG (negative control antibody) at the enhancer and promoter regions of the *Fam60a* gene. All ChIP enrichments are presented as the percentage of protein bound normalized to input. The promoter region of *Lipf* gene is included as a negative control.

D *Fam60a* mRNA level decreases upon depletion of Oct4 in mouse ES cells. RT–qPCR for *Fam60a* and *Oct4* mRNA levels in ES cells infected with either sh*Oct4* or scrambled control shRNA (shNT). Cells were harvested 48 h following selection.

Data information: In (B, C and D) the means ± SD of three technical replicates of a representative experiment is shown.
Source data are available online for this figure.

To understand the binding pattern of Fam60a on individual gene loci, we generated representative genome browser tracks depicting the co-occupancy of Fam60a together with Fam60a-Sin3a complex components and polymerase II on the H3K4me3-positive promoters of the *Ttc9*, *Per2*, *Sgpl1* and *Elf2* genes (Fig 4D). Interestingly, Fam60a, polymerase II and other Sin3a complex components also bind at an intergenic promoter within the *Elf2* gene locus, which perfectly overlaps with an H3K4me3 peak. This

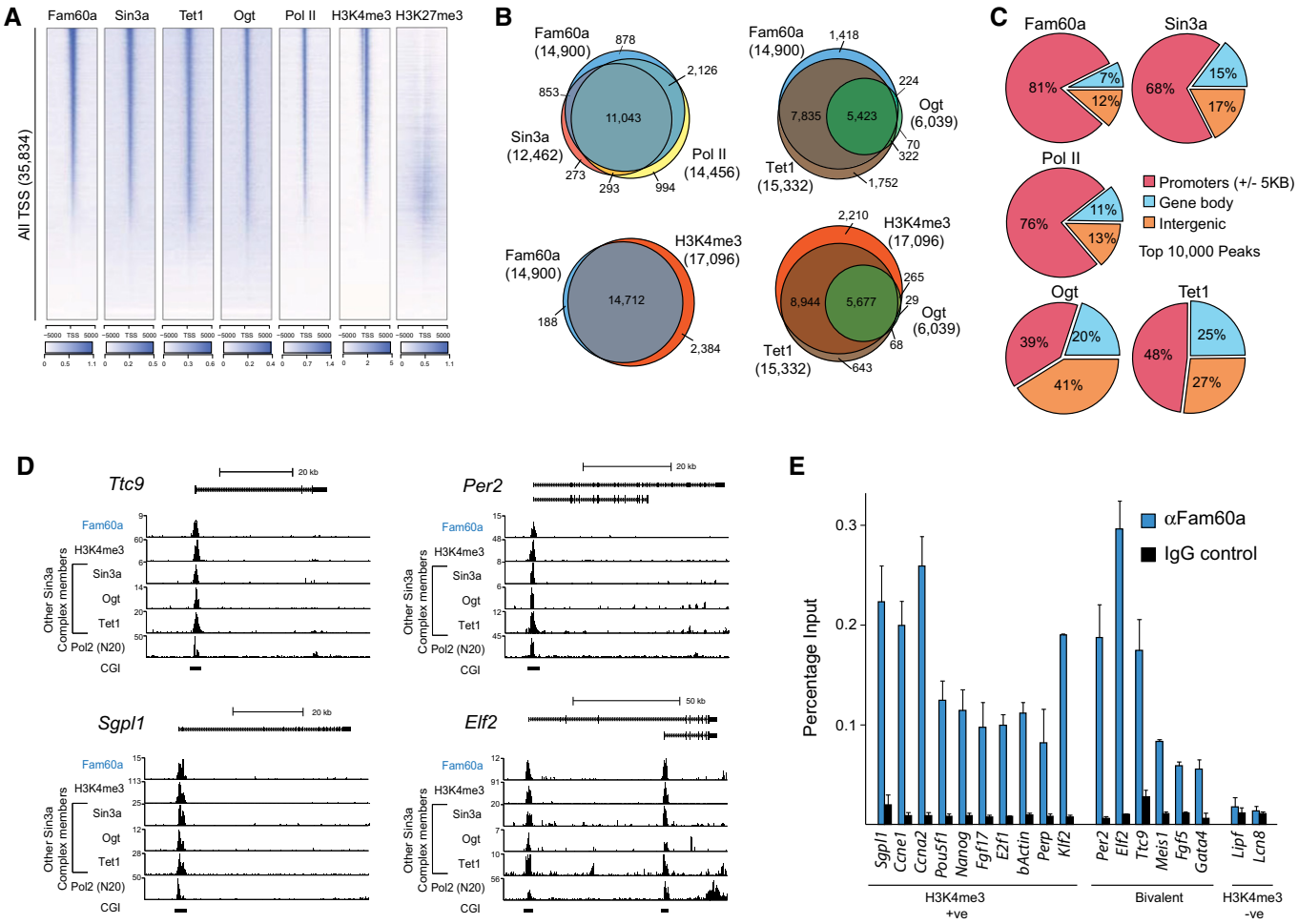

Figure 4. Fam60a co-occupies H3K4me3-positive promoters with Sin3a in mouse embryonic stem cells.

A Heatmap analysis representing ChIP-Seq of Fam60a and previously published ChIP-Seq data sets for Sin3a, Tet1, Ogt, RNA polymerase II and the histone modifications H3K4me3 and H3K27me3 (Williams *et al*, 2011; Vella *et al*, 2013; Denissov *et al*, 2014; Riising *et al*, 2014) in mouse ES cells. The sequence reads 5,000 bp up- and downstream of the transcriptional start site are shown, and the relative intensities are indicated in blue.

B Venn diagram analysis representing the number of common target gene promoters between Fam60a, Sin3a, H3K4me3, polymerase II, Tet1 and Ogt.

C Pie charts representing the distribution of the binding of Fam60A and the indicated other proteins at gene promoters, gene bodies and intergenic regions.

D Enrichment tracks of Fam60a, H3K4me3, Sin3a, Ogt, Tet1 and Pol II at the four representative Fam60a/Sin3a target genes: *Ttc9*, *Per2*, *Sgpl1* and *Elf2*. The gene structure and dimensions are indicated at the top of each panel, while the locations of CpG islands are presented by a black bar at the bottom.

E Quantitative ChIP analyses of Fam60a binding to both monovalent (H3K4me3 only) and bivalent (both H3K4me3 and H3K27me3) Fam60a/Sin3a target genes. The IgG antibody was included as a negative control. ChIP enrichments are presented as the percentage of protein bound normalized to input. The two genes *Lipf* and *Lcn8*, which both lack H3K4me3 at their promoter, are included as negative controls. The means ± SD of three technical replicates of a representative experiment is shown.

suggests that the minority of Fam60a, Sin3a and polymerase II binding away from promoters, observed in Fig 4C, could include non-annotated transcriptional start sites. Next, we performed ChIP-Seq analysis for Fam60a and Sin3a in immortalized mouse NIH3T3 fibroblasts (Fig EV2A and B). As expected, this revealed only residual binding of Fam60a at target genes in fibroblasts, whereas Sin3a, although not enriched as strongly as in ES cells, was still present on its target genes. Finally, we performed ChIP-qPCR validation analysis in ES cells to confirm the presence of Fam60a at both all H3K4me3-positive monovalent (10 of 10) and bivalent promoters (5 of 5) tested, but not on the promoters of H3K4me3-negative (2 of 2) genes (Fig 4E). Taken together, these data establish Fam60a as being bound together as part of the Fam60a-Sin3a complex to H3K4me3-positive promoters in ES cells, but not in more differentiated cells, suggesting it might have a particular role in ES cells.

Fam60a maintains Sin3a on target gene promoters in ES cells, and its loss leads to deregulated gene expression

We next wished to determine whether loss of Fam60a would have consequences for the Sin3a association with its target gene promoters. To do this, we infected ES cells with lentiviruses expressing two independent shRNAs that stably target *Fam60a* and observed the global reduction in Sin3a on chromatin (Fig EV3A–C). Next, ChIP-Seq suggested that Sin3a is strongly diminished genomewide on its

target gene promoters upon loss of Fam60a (Fig 5A). Since ChIP-Seq is not quantitative, we validated these observations by performing ChIP-qPCR analyses of both Fam60a and Sin3a at their target gene promoters in control versus Fam60a-depleted cells, using histone H3 and IgG as controls (Figs 5B and EV3D). This analysis also confirmed the specificity of the Fam60a antibody. Interestingly, while Fam60a is required for the stability of Sin3a in ES cells, its ectopic expression in ES cells or fibroblasts was not sufficient to stabilize Sin3a (Fig EV3E and F), indicating that Fam60a is essential, but not sufficient on its own, to stabilize the Sin3a complex. In conclusion, Fam60a is an essential component of the Fam60a-Sin3a complex required to maintain Sin3a levels on target gene promoters in ES cells.

To determine whether loss of Fam60a phenocopies the loss of Sin3a in terms of gene expression changes, we performed differential gene expression analysis following shRNA-mediated depletion of Fam60a and Sin3a, separately, and overlapped all commonly up- or down-regulated genes with those directly bound by both Fam60a and Sin3a (Fig 6A). This revealed that of the 11,896 direct Fam60a/Sin3a target genes, only 676 (6.2%) were significantly up- and 406 (3.8%) were down-regulated in both the Fam60a- and Sin3a-depleted cells (Table EV4). This is analogous to the few gene expression changes observed in cells depleted of the Polycomb chromatin regulators (Bracken *et al*, 2006) and might reflect the availability (or lack) of DNA-binding transcriptional regulators for many of these genes. A gene ontology analysis of the genes deregulated in the Fam60a- and Sin3a-depleted cells revealed enrichments for pathways with roles in cellular homeostasis and metabolism (Fig EV4A). In particular, the TGFβ pathway was enriched in the down-regulated gene set (Fig EV4A). Importantly, this pathway is known to have important roles in both the maintenance of ES cell pluripotency and during subsequent lineage specification and mesendodermal differentiation (Park, 2011; Itoh *et al*, 2014). Consistent with this, both the RNA-Seq (Fig 6B and C) and validatory RT–PCRs on an

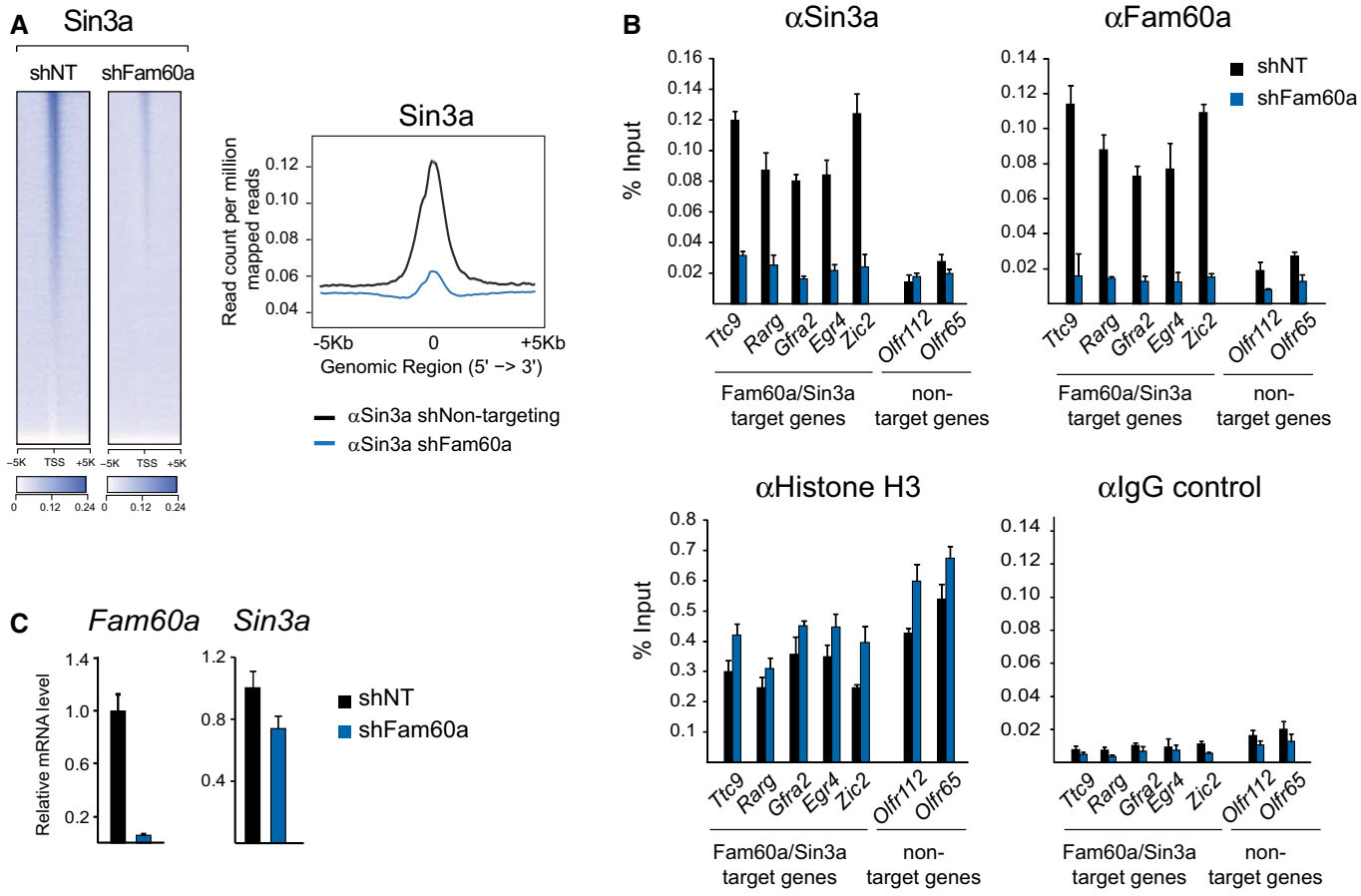

Figure 5. Fam60a is required to maintain Sin3a on target genes in ES cells.

A Heatmap presentation of Sin3a ChIP-Seq done in control or Fam60a-depleted ES cells. The sequence reads 5,000 bp up- and downstream of the transcriptional start site are shown, and the relative intensities are indicated in blue. The right panel presents the average profile of Sin3a binding regions in control versus Fam60a-depleted cells.

B ChIP-qPCR analyses using the indicated antibodies in mouse ES cells. Precipitated DNA was analysed by qPCR using primers directed towards the promoters of the indicated genes. ChIP enrichments are presented as the percentage of protein bound normalized to input. The means ± SD of three technical replicates of a representative experiment is shown.

C Quantitative RT–PCR analysis of the mRNA levels of *Fam60a* and *Sin3a* in control and Fam60a-depleted ES cells. The means ± SD of three technical replicates of a representative experiment is shown.

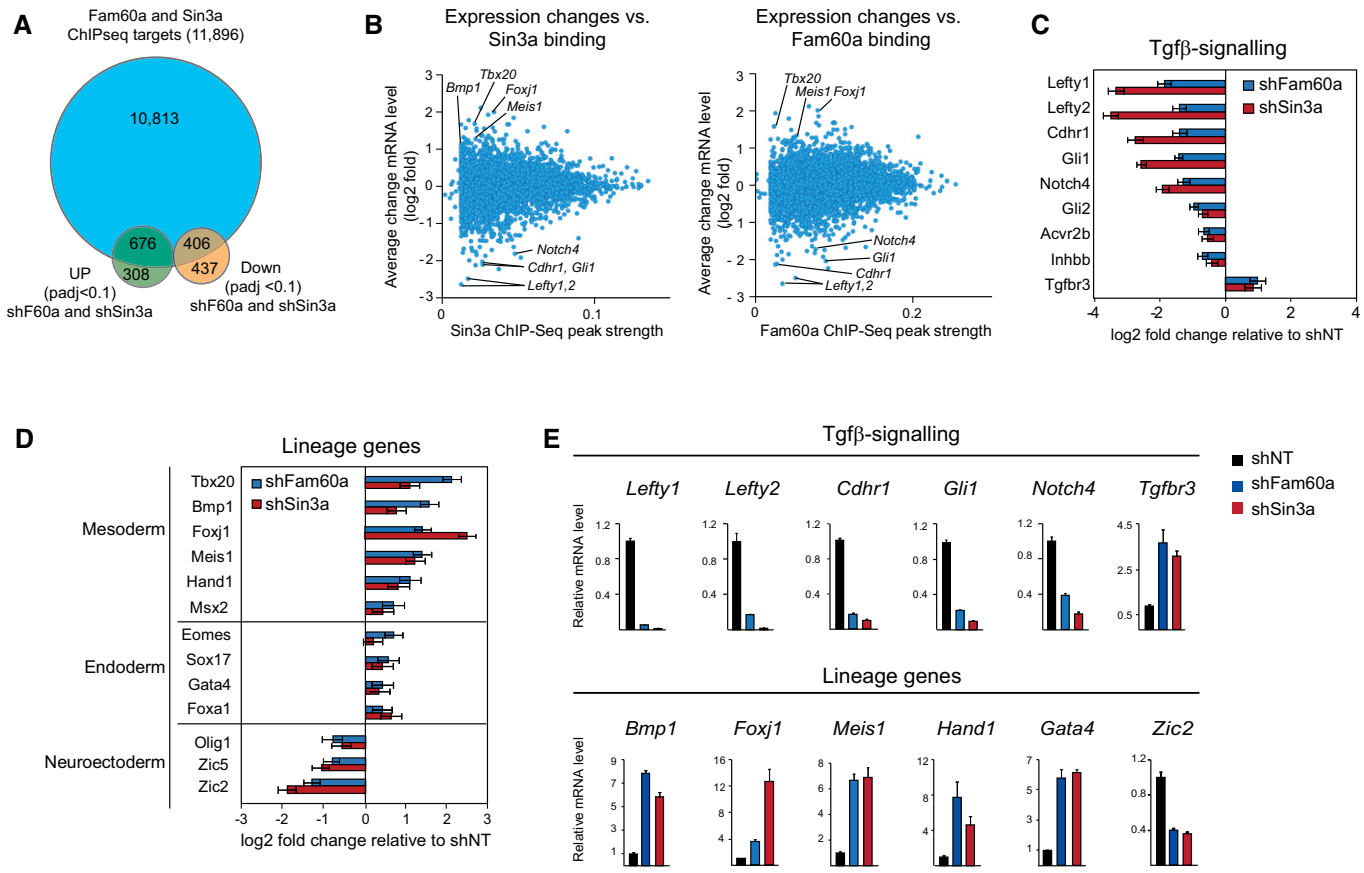

Figure 6. Loss of both Fam60a and Sin3a causes deregulation of a subset of their direct target genes.

A Venn diagram analysis representing the overlap of all genes directly bound by both Fam60a and Sin3a with those genes either up- and down-regulated in both the Fam60a- and Sin3a-depleted ES cells (biological replicates n = 3, adjusted P-value < 0.1). These differentially expressed genes were obtained by performing RNA-Seq on ES cells with shRNA-mediated knockdown of Fam60a and Sin3a, compared to non-targeting control (shNT), respectively. P-values were calculated using *DESeq2*, and Benjamini–Hochberg False Discovery Rate adjustment was applied.

B Dot plots representing the average mRNA expression changes as log2 fold change following Fam60a and Sin3a knockdowns relative to shNT control over the Sin3a (left) and Fam60a (right) ChIP-Seq peak strength. The genes *Tbx20*, *Foxj1*, *Meis1*, *Lefty1*, *Lefty* 2, *Cdhr1*, *Gli1* and *Notch4* are highlighted.

C The graphs represent log2 fold changes in mRNA levels of genes encoding members of the TGFβ signalling pathway following depletion of Fam60a and Sin3a relative to the shNT control. Data are based on RKPM (reads per kilobase per million mapped reads) obtained by RNA-Seq. The data of three biological replicates are presented as mean ± SD.

D As in (C). Graph shows genes encoding representative members of the mesodermal, endodermal and ectodermal lineages, as indicated.

E RT–qPCR of selected TGFβ pathway and lineage genes to validate the mRNA expression changes following Fam60a and Sin3a depletions in ES cells. The data of three technical replicates are presented as mean ± SD.

independent experiment (Fig 6E), revealed that the strongest deregulated genes in both the Fam60a- and Sin3A-depleted cells encoded key members of the TGFβ signalling pathway, among them *Lefty1, Lefty2, Cdhr1, Gli1* and *Notch4* (Fig 6C). Moreover, several of the up-regulated genes in both the Fam60a- and Sin3A-depleted cells represented mesodermal markers, including *Tbx20*, *Meis1* and *Foxj1*, whereas the down-regulated genes included markers of neuroectodermal lineage (Fig 6B, D and E). In contrast, neither the depletion of Fam60a or Sin3a affected the mRNA levels of the core pluripotency genes, including *Oct4*, *Nanog*, *Klf4* or *Sox2*, or E2f cell cycle genes (Fig EV4B and C), while other genes that have been associated with the pluripotent state, such as *Prdm14*, *Klf2* and *Pou2f3* (Pasini *et al*, 2007; Yamaji *et al*, 2013; Yeo *et al*, 2014), were down-deregulated. Moreover, we did not observe changes in Oct4 protein levels following depletion of Fam60a or Sin3a (Fig EV4D). In summary, Fam60a and Sin3a co-regulate common target genes with essential roles in cellular pathways central to ES maintenance, consistent with a shared function as part of the Fam60a-Sin3a complex.

Fam60a phenocopies Sin3a in its requirement for rapid proliferation of ES cells

Previous reports showed that cells of the inner cell mass of Sin3a knockout blastocysts failed to proliferate *in vitro* (Cowley *et al*, 2005), and a conditional knockout of Sin3a in ES cells led to defects in cell cycle and survival (McDonel *et al*, 2012). To determine whether depletion of Fam60a would phenocopy the loss of Sin3a, we first performed colony formation assays of ES cells cultured in serum and LIF containing medium, following stable knockdown of either Fam60a or Sin3a (Fig 7A). The colony morphology typical of undifferentiated ES cells was lost in both

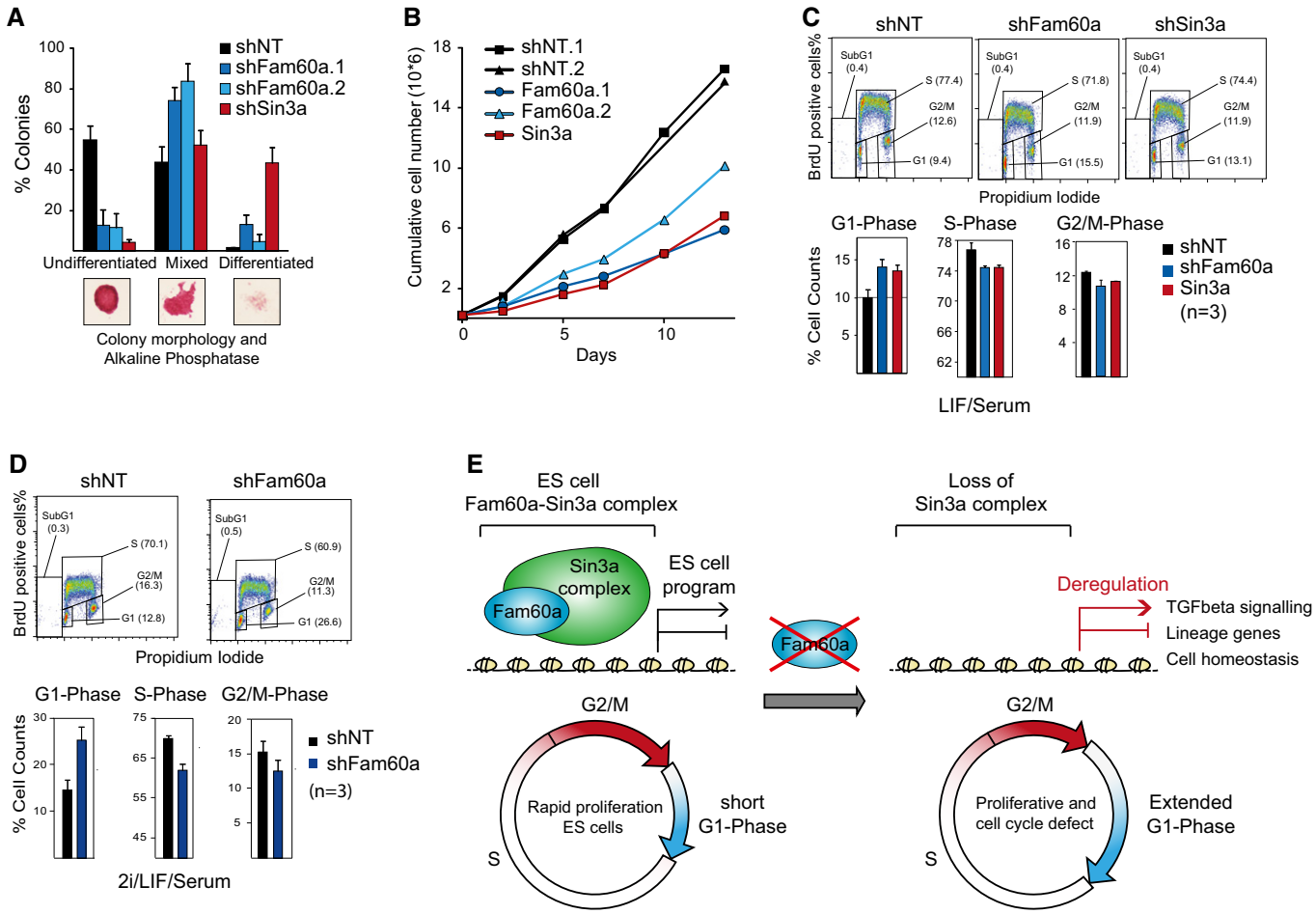

Figure 7. Loss of both Fam60a and Sin3a causes differentiation, proliferation and cell cycle defects in ES cells.

A Colony formation assays with alkaline phosphatase staining of ES cells that were transfected with two shRNAs targeting Fam60a, a shRNA targeting Sin3a and a non-targeting control shRNA. Representative images below the graph represent colonies of undifferentiated, mixed differentiated and differentiated colonies. The assays were performed in biological triplicates and are presented as mean ± SD.

B Growth curve of ES cells following depletion of Fam60a or Sin3a. Two different negative control shRNA vectors shNT.1 (non-targeting control pLKO.TRC1SCR) and shNT.2 (non-targeting control pLKO.TRC2SCR) were used.

C BrdU and propidium iodide FACS analysis (indirect method) to monitor the cell cycle changes in Fam60a- and Sin3a-depleted ES cells. The upper panel shows representative FACS plots for each knockdown condition and the control shRNAs (pLKO.TRC2SCR). Percentage of cell numbers of SubG1, G1, S and G2/M phase are shown. The data of three biological replicates are presented as mean ± SD.

D As in (C). BrdU and propidium iodide FACS analysis (indirect method) to monitor the cell cycle following Fam60a depletion in ES cells grown in 2i/LIF.

E Model of the role of Fam60a within the Sin3a complex in ES cells. The presence of Fam60a in the Sin3a complex maintains it on chromatin and ensures rapid ES cell proliferation, a short G1-phase and a proper ES cell gene expression program. The loss of Fam60a leads to slowed cellular proliferation, an extended G1-phase of the cell cycle and a deregulation of the ES cell gene expression program.

the Fam60a and Sin3a knockdowns, with most colonies displaying differentiated morphologies. Next, we performed cell growth assays and found that depletion of Fam60a phenocopied the loss of Sin3a in both LIF/Serum (Fig 7B) and 2i/LIF/Serum media (Fig EV5A).

Previous work established that a rapid proliferation rate and a short G1-phase of the cell cycle are defining features of ES cells (Kareta *et al*, 2015; Boward *et al*, 2016) and that lineage priming in these cells is intrinsically linked to their G1-phase during which they become more susceptible to differentiation (Calder *et al*, 2013; Coronado *et al*, 2013). Therefore, we next wished to investigate whether the reduced proliferation rate and increased differentiation phenotype upon depletion of Fam60a and Sin3a might be linked to an altered cell cycle in these cells. We performed BrdU labelling, combined with propidium iodide FACS, and found that depletion of both Fam60a and Sin3a led to an extended G1-phase and reduced S and G2/M-phases in both LIF/Serum and 2i/LIF/Serum conditions (Figs 7C and D, and EV5B). The proportion of cells in SubG1 was unchanged, indicating that apoptosis was not the reason for the decreased proliferation rates. Taken together, these data suggest that cells with reduced levels of Fam60a or Sin3a spend more time in the G1-phase. Since this defect was accompanied by the up-regulation of mesodermal lineage marker genes, it suggests that the role Fam60a in maintaining the undifferentiated state is intrinsically linked to its roles in ensuring rapid cellular proliferation.

Overall, these experiments establish that Fam60a is a crucial component of a variant Sin3a chromatin complex in ES cells, required to promote rapid proliferation and to maintain ES cells in an undifferentiated state (Fig 7E).

Discussion

This work for the first time systematically compares the endogenous stoichiometric composition of the prototypical Sin3a Hdac/2 complex in embryonic stem (ES) and differentiated cells. We find that Sin3a complexes undergo dynamic compositional changes during cellular differentiation. Our key findings are that we identify a variant Sin3a-Hdac complex, Fam60a-Sin3a, that is predominantly present in ES cells, and that Fam60a is essential for the function of this Sin3a complex. Crucially, Fam60a as a defining subunit of the Fam60a-Sin3a complex is required to maintain key features of ES cells, including rapid cellular proliferation, and the prevention of unscheduled differentiation.

Recent advances in mass spectrometry-based technologies have now enabled the exploration of multi-protein chromatin regulator complexes in different biological contexts (Aebersold & Mann, 2016). However, the majority of protein interaction network studies use tagging strategies, which risk to create artefacts due to interference with the normal protein network (van Nuland *et al*, 2013; Kloet *et al*, 2016). To avoid this issue, we developed an approach to couple two independent endogenous immunoprecipitations with quantitative mass spectrometry, thereby allowing us to identify subtle variations in the composition of the Sin3a-Hdac complex during the process of cellular differentiation of ES cells. Using this approach, we discover a variant of the Sin3a core complex composition in ES cells, which is defined by an almost stoichiometric ratio of the Fam60a protein relative to Sin3a. Supporting a central role of the Fam60a protein in the Sin3a complex of ES cells, we find that it co-occupies the majority of H3K4me3-positive gene promoters together with Sin3a genome-wide. In addition to the core Fam60a-Sin3a complex, composed of Fam60a, Sap30, Hdac1 and Rbbp4/7, several additional Sin3a accessory proteins, such as Ing1 and Ing2, Brms1 and Brms1l, were also detected in the Sin3a immunoprecipitations, albeit with lower stoichiometries, suggesting the existence of multiple different combinations of the complex. Supporting this, the Sin3a complex sediments with broad elution profiles (400 kDa to 2 MDa) in size exclusion chromatography experiments (Skowyra *et al*, 2001; Kuzmichev *et al*, 2002). Furthermore, a previous study provided evidence that homologous proteins such as Brms1 and Brms1L, Ing1 and Ing2, are mutually exclusive in the complex (Sardiu *et al*, 2014). Therefore, while we define Fam60a as a core member of Sin3a complexes in ES cells, further functional and genomewide studies of other sub-stoichiometric subunits will be required to decipher their respective contributions.

Tet1 and Ogt are two sub-stoichiometric Fam60a-Sin3a complex members that we show to specifically associate in ES cells, albeit with lower stoichiometries relative to Fam60a. This is again consistent with our finding that the Sin3a complex has a special composition in ES cells and with previous reports, which showed that Tet1 and Ogt associate with the Sin3a protein in ES cells (Yang *et al*, 2002; Williams *et al*, 2011). However, the fact that Ogt and Tet1 have low enrichments in the Sin3a complex suggests that they do not form stable physical interactions with the Sin3a complex at their common genomic target regions. Interestingly, while Tet1 and Ogt co-bind together with Fam60a and Sin3a on the majority of H3K4me3-positive promoters, they also bind at intergenic regions, independently of the Sin3a complex, suggesting they have roles independent of the Sin3a complex. Our data are consistent with a previous report showing that most Ogt binding sites are co-occupied by Tet1 and that these two proteins physically associate with each other (Vella *et al*, 2013). Furthermore, a role for Tet1 in promoting the presence of Sin3a on chromatin, in addition to its activity to generate 5-hydroxymethyl cytosine, was previously reported (Williams *et al*, 2011; Wu *et al*, 2011). Taken together with our results, we speculate that, unlike Fam60a, Ogt and Tet1 are part of additional chromatin complexes and that their association with the Fam60a-Sin3a complex is a particular aspect of ES, but not of differentiated cells.

While the Sin3a complex has generally been regarded to be a transcriptional repressive complex, our results are consistent with several recent lines of evidence suggesting that, in general, Hdac1/2 containing complexes play roles in both transcriptional activation and repression (Reynolds *et al*, 2013; Baymaz *et al*, 2015). For example, we find that the disruption of the Fam60a-Sin3a complex in ES cells leads to an approximately equal distribution of up- and down-regulation of direct target genes. This is in line with our demonstration that both Fam60a and Sin3a bind genomewide to promoters marked with H3K4me3, which is a histone post-translational modification associated with both active and poised genes. Notably, although the Sin3a complex was first described in yeast as being a transcriptional repressor and associated with histone deacetylation activity (Vidal *et al*, 1991), it has also been reported to be required for the transcriptional activation of genes induced by osmotic stress and by heat shock in yeast (De Nadal *et al*, 2004; Ruiz-Roig *et al*, 2010). Moreover, in mammals, Sin3a was found on a subset of actively transcribed muscle genes in myoblasts and shown to be required to maintain their expression (van Oevelen *et al*, 2010). Furthermore, in agreement with our data, both histone acetyltransferases and Hdacs have been reported to bind at the promoters of actively transcribed genes as well as non-transcribed genes with the H3K4me3 mark (Wang *et al*, 2009). Studies in synchronized breast cancer cells led to a model of cyclical regulation of active transcription in which cycles of acetylation and deacetylation are regulated by cyclical binding of HATs and Hdacs, thereby potentially providing insights into the role of Hdac containing complexes in gene activation (Metivier *et al*, 2003).

Towards deciphering the particular role of Fam60a within the Sin3a complex, we show here that it is required to maintain the stability of the Sin3a protein in ES cells. Consistent with the lack of Fam60a in differentiated lineages, Sin3a is less enriched on its target gene promoters in mouse fibroblasts, which have lower Fam60a levels. In terms of how the Fam60a-Sin3a complex locates to H3K4me3-positive gene promoters, the two sub-stoichiometric components, Ing1 and Ing2, have been reported to promote binding via their H3K4me3 reader domains (Shi *et al*, 2006; Cheng *et al*, 2014). However, the Fam60a protein has a predicted Gata-like Zinc finger domain in its N-terminus, and it will therefore be interesting to determine whether it is directly

involved in DNA binding and/or tethering the Sin3a complex to chromatin (Munoz *et al*, 2012). This would be consistent with the model of multivalent interactions of the multi-protein chromatin regulator complexes with chromatin and the underlying DNA (Allis & Jenuwein, 2016). It will be important to further explore the molecular mechanisms by which Fam60a contributes to Sin3a complex function in ES cells. Recently, Sin3a was reported to interact with Nanog to promote the pluripotency (Saunders *et al*, 2017). However, we did not detect Nanog in our Sin3a or Fam60a immunoprecipitations and believe any Sin3a–Nanog interaction would be indirect and dependent on colocation on chromatin. Similarly, while we detect the DNA-binding factors (Foxk2 and Mxi1) in the Sin3a complex in differentiated cells, there is no evidence they target the complex, especially considering their very low stoichiometries. It will be interesting to evaluate whether they have any direct or indirect role in the recruitment of the Sin3a complex to its target genes in differentiated cells. Taken together, the association of the Sin3a complex to its target gene promoters is likely promoted by the combinatorial action of several histone and non-sequence-specific DNA affinities.

Our results have implications for the potential role of Fam60a and the Sin3a complex in other rapidly proliferating cells, including cancer. Consistent with *Fam60a* being a potential E2f regulated gene, we find that its mRNA levels are high in rapidly proliferating ES cells and down-regulated during differentiation, as proliferation slows. While further characterization of the transcriptional regulation of Fam60a is required, our data are consistent with the previously reported cell cycle regulation of *Fam60a* mRNA levels in U2OS cancer cells (Munoz *et al*, 2012). Intriguingly, the human FAM60A protein is highly expressed in several cancer cell lines and co-purifies with Sin3a (Smith *et al*, 2012), suggesting that *FAM60A* mRNA levels might be up-regulated in cancer cells due to its transcriptional activation by E2F, which is deregulated in most cancer cells (Lanigan *et al*, 2011). This raises the question as to whether *FAM60A* is also highly expressed in other rapidly proliferating normal cells such as tissue-specific progenitors. Therefore, it will be interesting to explore the role of FAM60A for the proliferative potential of both in normal rapidly proliferating progenitor cells and in cancer. Consistent with a key role for Fam60a in regulating cellular proliferation, we have shown that its depletion in ES cells phenocopies the loss of Sin3a, leading to a reduced rate of cellular proliferation. This is in accordance with previous reports that loss of Sin3a in mouse fibroblasts and ES cells leads to defects in cellular proliferation, concomitant with reduced numbers of cells in S-phase and an accumulation in G2/M phase (Cowley *et al*, 2005; Dannenberg *et al*, 2005; McDonel *et al*, 2012). Thus, the Fam60a-Sin3a complex may be intrinsically linked with rapid cellular proliferation, and as such, it is likely deregulated in human cancer.

To summarize, we find that the composition of the endogenous Sin3a-Hdac1/2 complex changes during cellular differentiation and that Fam60a defines a variant "Fam60-Sin3a complex" present in ES cells, which we link to the control of cellular proliferation. This work establishes an important link between the dynamic changes in the composition of the multi-protein Sin3a Hdac1/2 complex and its roles in the control of cellular proliferation, pluripotency and cell fate decisions.

Materials and Methods

Cell culture and lentiviral transduction

Embryonic stem cells were grown on gelatinized culture dishes in GMEM media (Sigma-Aldrich) supplemented with 10% FBS (Gibco) (v/v), 1,000 U/ml leukaemia inhibitory factor (EMD-Millipore), 100 U/ml penicillin, 100 U/ml streptomycin (Gibco), 1:100 GlutaMAX (Gibco), 1:100 non-essential amino acids (Gibco), 1 mM sodium pyruvate (Gibco) and 50 μM β-mercaptoethanol (Sigma-Aldrich). NIH3T3 and NTERA-2 cells were grown in DMEM media supplemented with 10% FBS (Hyclone), 100 U/ml penicillin and 100 U/ml streptomycin (Gibco). NTERA-2 cells were differentiated by addition of 10 μM all-trans retinoic acid to the growth medium and harvested at 70% confluency. For transfection of cells with shRNA, lentiviral particles were produced and used to transduce target cells as previously described (Brien *et al*, 2012). Cells were selected with puromycin for 3–5 days before seeded for assays. All shRNA sequences are available in Table EV5.

Embryonic stem cell differentiation

Embryoid body differentiation of ES cells was induced by plating 1×10^5 cells/ml in non-adherent bacterial dishes (Greiner) in ES cell media without LIF. The media was changed every 2 to 3 days throughout the differentiation procedure.

Colony formation and alkaline phosphatase staining

Cells were seeded at low density in 12-well plates and grown for 5 days. Then, the cells were fixed with 4% paraformaldehyde in PBS and used for alkaline phosphatase staining to visualize ES cell colonies, according to the manufacturer's protocol (EMD-Millipore, Alkaline Phosphatase Detection Kit; SCR004).

Antibodies

The following antibodies were used: sheep αFam60 (a kind gift from John Rouse), rabbit αSin3a (Abcam, ab3479), Sin3a (Santa Cruz, sc-994), rabbit αH3 (Abcam, ab1791). Ogt (Santa Cruz, sc-32921), Oct4 (Abcam, ab19857), Hdac1 (Santa Cruz, sc-81598), Cbx8 (Bracken *et al*, 2006), beta-tubulin (Santa Cruz, sc-9104), beta-actin (Thermo Fisher, AC-15). For Flag-IPs, anti-Flag M2 affinity Agarose Gel (Sigma-Aldrich, A2220) was used. For control immunoprecipitations, either normal rabbit IgG (EMD-Millipore, 12-270) or total sheep IgG (Santa Cruz, sc-2717) was used. HRP-linked secondary antibodies anti-rabbit (Sigma-Aldrich, A0545), anti-mouse (Merck, 401253), anti-goat (Santa Cruz, sc-2020) and anti-sheep (EMD-Millipore, 12-342) were used.

Endogenous immunoprecipitations

For endogenous Sin3a-IPs, the antibodies Sin3a.1 (Abcam, ab3479), Sin3a.2 (Santa Cruz, sc-994) and rabbit total IgG (EMD-Millipore, 12-370) were used. For Fam60a endogenous IPs, the antibodies Fam60a (a kind gift from John Rouse (Munoz *et al*, 2012) and total sheep IgG (Santa Cruz, sc-2717) were used.

Immunoprecipitations were performed as previously described (van den Berg *et al*, 2010). Briefly, nuclear pellets were lysed in Buffer C containing protease inhibitors (20 mM HEPES (pH 7.6), 20% (v/v) glycerol, 0.42 M NaCl, 1.5 mM $MgCl_2$, 0.2 mM EDTA, aprotinin 1 μg/ml, leupeptin 10 μg/ml, PMSF 1 mM) and subsequently dialysed against Buffer C-100 (20 mM HEPES (pH 7.6), 20% (v/v) glycerol, 0.2 mM EDTA, 100 mM KCl, 1.5 mM $MgCl_2$, 0.2 mM EDTA). A total of 10 μg of antibody was coupled with beads and then incubated with 1 ml of dialysed nuclear extracts (usually 1.5–2 mg protein) containing 250 units/ml of benzonase (Sigma-Aldrich) for 4 h at 4°C, in order to prevent the detection of nucleic acid-mediated indirect false-positive protein interactions. Beads were then washed five times with Buffer C100 supplemented with 0.02% NP-40 and one time with 1× PBS. The bead-bound protein complex was directly tryptically digested and used for sample preparation for mass spectrometry as previously described (Oliviero *et al*, 2015). For Western blot analysis, beads were eluted with 2× SDS loading dye. Flag-M2 (Sigma-Aldrich, A2220)-bound proteins were eluted with 250 μg/ml Flag peptide (Sigma-Aldrich, F4799) for Western blot analysis.

Mass Spectrometry and data analysis

Immunoprecipitated samples were directly processed for digestion with trypsin (Promega), as described previously (Wisniewski *et al*, 2009). The samples were then analysed by LC-MS, as we described previously (Oliviero *et al*, 2015). The peptides were analysed with a Q-Exactive mass spectrometer via an EASY-nLC 1000 HPLC system (Thermo Fisher) coupled with an in-house packed C18 column (New Objective). Parent ion spectra (MS1) were measured at resolution 70,000, AGC target 3e6. Tandem mass spectra (MS2; up to 10 scans per duty cycle) were obtained at resolution 17,500, AGC target 5e4, collision energy of 25. Mass spectrometry data were processed using MaxQuant version 1.3.0.5 (Cox & Mann, 2008) using the mouse UniProt database (Download June 20115, 76,086). The following search parameters were used: Fixed Mod: cysteine carbamidomethylation; Variable Mods: methionine oxidation; Trypsin/P digest enzyme (maximum two missed cleavages); Precursor mass tolerances 6 ppm; Fragment ion mass tolerances 20 ppm; Peptide FDR 1%; Protein FDR 1%. "Label-Free Quantitation; LFQ", "iBAQ", and "Match Between Run" settings were selected. Reverse hits and contaminants were filtered, and the Perseus program (http://coxdocs.org; Tyanova *et al*, 2016) was used to carry out statistical analysis. Briefly, the LFQ values were transformed (log2) and missing values imputed to a normal distribution (width = 0.3; shift = 1.8), and a two-tailed *t*-test applied with correction for multiple testing. To determine relative stoichiometries, the iBAQ method was performed, as previously described (Smits *et al*, 2013). To do this, the average iBAQ values of all Sin3a immunoprecipitations were used and subtracted from the average iBAQ values of the IgG controls. As cut-off for protein enrichments in the ES or differentiated cells, proteins were defined as enriched when at least twofold difference between ES and EBs and a more than threefold difference between ES and fibroblasts was measured. Volcano plots were generated using Perseus software (1.4.1.3), version 1.4, as previously described (Smits *et al*, 2013). The two-sample *t*-test compared to IgG control was performed with a false discovery rate (FDR) 0.01.

Western blotting

Total protein lysates were generated by lysing cells in IPH buffer (50 mM Tris pH 8.0, 150 mM NaCl, 5 mM EDTA, 0.5% NP-40 and protease inhibitors 2 μg/ml aprotinin, 1 μg/ml leupeptin, 10 μg/ml PMSF and 0.5 mM DTT). To obtain chromatin-associated proteins, the lysates were incubated with Benzonase (125 U/mg protein) with addition of 7 mM $MgCl_2$ (final 2 mM) at 4°C. For Western blotting, all protein lysates were separated on SDS–PAGE gels and transferred to nitrocellulose membranes. Membranes were subsequently probed using the relevant primary and secondary antibodies, and relative protein levels were determined by chemiluminescence.

Chromatin immunoprecipitation

ChIP analyses were performed as described previously (Bracken *et al*, 2006). Briefly, formaldehyde cross-linked chromatin was sheared to 200–1,000 bp by sonication. Chromatin was incubated overnight at 4°C with the indicated antibodies. A total of 3 μg of antibodies specific for Fam60a (a kind gift from John Rouse, Munoz *et al*, 2012), Sin3a (Abcam, ab3479) and total sheep IgG (Santa Cruz, sc-2717) and rabbit IgG (EMD-Millipore, 12-370) were used. For ChIPs of histone H3, 1 μg of anti-histone H3 antibody (Abcam, ab1791) was used. After incubation, the immunoprecipitates were isolated using protein A or G Sepharose beads (Sigma-Aldrich). The beads were then washed, eluted and the DNA purified by phenol/chloroform extraction and ethanol precipitation prior to quantitative PCR and/or sequencing analyses.

ChIP-Seq library preparation and sequencing

All immunoprecipitated DNA was quantified using the Qubit® dsDNA HS Assay Kit (Invitrogen). A total of 1–5 ng DNA from ChIP experiments was used for library preparation using the Illumina ChIP-Seq sample prep kit (Illumina, IP-102-1001) and multiplexing oligonucleotide kit (Illumina, PE-400-1001). Following adaptor ligation, DNA was PCR amplified for 15 cycles. The DNA was purified using a DNA SPRI bead (Beckman Coulter) cleanup approach. The quality of the DNA libraries was assessed using a high-sensitivity Bioanalyzer Chip (Agilent Technologies). Libraries were used for cluster generation and sequencing using HiSeq 2000 (Illumina) at a 50-bp read length.

Bioinformatic analysis of ChIP-Seq data

Sequencing data were aligned to the mouse reference genome (mm10) using Bowtie2 (Langmead & Salzberg, 2012). Peaks were calculated using MACS2 (Zhang *et al*, 2008). Only peaks significant at a false discovery rate of 1% were considered in downstream analysis. Bigwig files were generated by first creating wig files using MACS1.4 and converting them to bigwig files using the wigToBigWig utility from UCSC. Bigwig files were smoothened within a 150-bp window using a custom script and tracks subsequently visualized using the UCSC genome browser. Heatmaps of read density and average binding profiles around transcription start sites (TSS) were produced using the program ngs.plot (Shen *et al*, 2014). The presence of Fam60a, Sin3a, Pol II, H3K4me3 peaks at TSSs were determined by computing the overlap of peaks

at the TSS ± 5 kb for each mm10 RefSeq annotated gene. The overlaps were computed using the program bedtools (v2.26.0), (Quinlan & Hall, 2010). The gene coordinates were retrieved from the UCSC table browser. Similarly, the proportion of Fam60a, Sin3a, Pol II, Ogt and Tet1 peaks occupying promoters (TSS ± 5 kb), gene bodies and intergenic regions were obtained by computing the overlap of the ten thousand most significant peaks based on FDR with these regions.

RNA sample preparation and RNA-Seq

A total of 1 μg of total RNA was used to generate libraries using the TruSeq Stranded mRNA Library Prep Kit (Illumina), as per the manufacturer's instructions. The library was assessed for overall quality using the Agilent High-Sensitivity DNA Kit with the Bioanalyzer 2100 (Agilent Technologies). The libraries were subsequently sequenced on the HiSeq 2500 v4.0 system (1 × 50 bp), (Illumina). For the bioinformatic analysis, raw sequencing data (as Fastq files) were aligned to the *Mus musculus* mm9/NCBI build 37 genome using STAR (2.4.0j), (Dobin *et al*, 2013). Read duplicates were removed using Picard Tools (v1.105; https://broadinstitute.github.io/picard/) using the default parameters. Differentially expressed genes (DEGs) were identified using DESeq2 (Love *et al*, 2014). An FDR adjusted = 0.1 was used to determine deregulated genes. Reads per kilobase per million reads (RPKMs) were generated to investigate absolute expression of genes.

Quantitative real-time PCR

Total RNA was extracted from cells using the RNeasy Purification Kit (Qiagen) and was used to generate cDNA by reverse transcriptase PCR using the TaqMan Reverse Transcription Kit (Applied Biosystems). Relative mRNA expression levels were determined using the SYBR Green I detection chemistry (Applied Biosystems). Data were analysed with the $\Delta\Delta C_T$ method, using a housekeeping gene as normalizer (*GAPDH, RPLPO*). For ChIP-qPCRs, enrichments were calculated relative to the C_t-values of Input, as indicated. Error bars represent the standard deviation of triplicate qPCR data. All qPCRs shown are representative results from a single experiment, which were performed multiple times. All primer sequences are available in Table EV5.

Growth curves

Embryonic stem cells were seeded at equal densities (2×10^5 cells per 6-well) and trypsinized when colonies reached 60–70% confluency. Cells were counted with a Neubauer chamber diluted 1:1 with trypan blue dye (Sigma-Aldrich) in order to discount dead cells.

Cell cycle analysis

BrdU and propidium iodide staining (indirect method) was performed, as previously described (Piunti *et al*, 2014). In short, cells were grown in the presence of 33 μM BrdU for 30 min and then fixed in 75% ice-cold ethanol, permeabilized with 2N HCl for 30 min at room temperature and pH equilibrated using 0.1 M BORAX (Sigma-Aldrich) for 2 min. Cells were incubated with a mouse anti-BrdU antibody (BD) in 1% BSA in 1× PBS for 1 h at room temperature, washed and stained with a donkey anti-mouse FITC-conjugated antibody (Jackson). Stained cells were treated with RNase A (Sigma-Aldrich) followed by DNA staining with 2.5 mg/ml propidium iodide (Sigma-Aldrich) overnight at 4°C . Intensities were acquired using BD FACS Calibur (BD Biosciences) and analysed using the FlowJo software.

Generation of stably Flag-Fam60a expressing ES cell lines and Flag-IPs

The mouse open reading frame of Fam60a was cloned from cDNA generated from mouse ES cell RNA into the pCR8 vector using the pCR8/GW/TOPO TA Cloning Kit, according to the manufacturer's guidelines (Thermo Scientific, K250020). Following sequencing, the ORF was cloned in the pCAG-Flag-Avi Gateway destination vector using Gateway LR Clonase Enzyme Mix (Thermo Scientific, 11791043). The pCAG-Flag-Avi-Fam60a and pCAG-Flag-Avi empty vector were lipofected in ES cells carrying stably the BirA expression vector pEF1BirAV5-neo (kind gift from Diego Pasini) and selected with 1.5 μg/ml puromycin. Cell colonies were screened for Flag-Fam60a expression compared to control cell lines. Two clones expressing Flag-Fam60a and two empty vector cell lines were used. The IPs were performed using Flag-M2 affinity gel under the same conditions as endogenous IPs (Sigma-Aldrich, A2220). Bead-bound protein complexes were tryptically digested and prepared for mass spectrometry.

Data availability

The mass spectrometry proteomics data have been deposited to the ProteomeXchange Consortium via the PRIDE partner repository with the data set identifier PXD005464. Raw data, including results files and software needed for viewing spectra, are provided. ChIP-Seq of Sin3a and Fam60a in E14 mouse ES and NIH3T3 cells and ChIP-Seq of Sin3a following shRNA-mediated knockdown of Fam60a in ES cells can be obtained from Gene Expression Omnibus, accession number GSE81081. The public ChIP-Seq data used in this paper were retrieved from GSM611194 for Tet1 and GSM611196 for Sin3a (Williams *et al*, 2011), GSM957084 for Ogt (Vella *et al*, 2013), GSM1258237 for H3K4me3 (Denissov *et al*, 2014) and for polymerase II and H3K27me3 (Riising *et al*, 2014). The RNA-Seq data can be obtained from Gene Expression Omnibus, accession number GSE87084.

Expanded View for this article is available online.

Acknowledgements

We thank members of the Bracken laboratory for helpful discussions and critical reading of the manuscript. We also thank Dr. John Rouse, University of Dundee, for providing the Fam60a antibody. We thank members of the Pasini Lab for the helpful support and Rut Klinger for help with the RNA-Seq sample preparation. S.D was supported by the Irish Cancer Society post-doctoral fellowship—CRF13DAS. Work in the Cagney Lab was supported by Science Foundation Ireland (SFI/10/1N.1/B3.19). Work in the Bracken Lab is supported by Science Foundation Ireland under the Principal Investigator Career Advancement Award (SFI/10/IN.1/B3002), the Health Research Board under the Health Research Awards 2010 (HRA_POR/2010/124), the Irish Research Council,

St. Vincent's Foundation and the Irish Cancer Society Collaborative Cancer Research Centre, and BREAST-PREDICT Grant, CCRC13GAL (www.breastpredict.com).

Author contributions

GS, GC and APB designed the research. GS performed and analysed the majority of the experiments. GO, AW, KW and GC processed mass spectrometry samples and MaxQuant analysis for Figs 1 and 2. NM and GC processed mass spectrometry samples for Appendix Fig S1. ETD and GLN helped with some of the proteomics computational procedures and uploading data to PRIDE. DP helped with sequencing of ChIP experiments. DJF generated graphs related to ChIP-Seq results in Figs 4, 5, and EV2. DJF, SJ and KH performed bioinformatics analyses of the CHIP-Seq data. AS helped with FACS analysis. BM performed bioinformatic analysis of the RNA-Seq. SD and DPO'C generated RNA-Seq libraries and performed the sequencing. GS and APB wrote the manuscript.

Conflict of interest

The authors declare that they have no conflict of interest.

References

Aebersold R, Mann M (2016) Mass-spectrometric exploration of proteome structure and function. *Nature* 537: 347 – 355

Alland L, David G, Shen-Li H, Potes J, Muhle R, Lee HC, Hou H Jr, Chen K, DePinho RA (2002) Identification of mammalian Sds3 as an integral component of the Sin3/histone deacetylase corepressor complex. *Mol Cell Biol* 22: 2743 – 2750

Allis CD, Jenuwein T (2016) The molecular hallmarks of epigenetic control. *Nat Rev Genet* 17: 487 – 500

Baymaz HI, Karemaker ID, Vermeulen M (2015) Perspective on unraveling the versatility of 'co-repressor' complexes. *Biochem Biophys Acta* 1849: 1051 – 1056

van den Berg DL, Snoek T, Mullin NP, Yates A, Bezstarosti K, Demmers J, Chambers I, Poot RA (2010) An Oct4-centered protein interaction network in embryonic stem cells. *Cell Stem Cell* 6: 369 – 381

Boward B, Wu T, Dalton S (2016) Concise review: control of cell fate through cell cycle and pluripotency networks. *Stem Cells* 34: 1427 – 1436

Bowman CJ, Ayer DE, Dynlacht BD (2014) Foxk proteins repress the initiation of starvation-induced atrophy and autophagy programs. *Nat Cell Biol* 16: 1202 – 1214

Bracken AP, Ciro M, Cocito A, Helin K (2004) E2F target genes: unraveling the biology. *Trends Biochem Sci* 29: 409 – 417

Bracken AP, Dietrich N, Pasini D, Hansen KH, Helin K (2006) Genome-wide mapping of Polycomb target genes unravels their roles in cell fate transitions. *Genes Dev* 20: 1123 – 1136

Brien GL, Gambero G, O'Connell DJ, Jerman E, Turner SA, Egan CM, Dunne EJ, Jurgens MC, Wynne K, Piao L, Lohan AJ, Ferguson N, Shi X, Sinha KM, Loftus BJ, Cagney G, Bracken AP (2012) Polycomb PHF19 binds H3K36me3 and recruits PRC2 and demethylase NO66 to embryonic stem cell genes during differentiation. *Nat Struct Mol Biol* 19: 1273 – 1281

Calder A, Roth-Albin I, Bhatia S, Pilquil C, Lee JH, Bhatia M, Levadoux-Martin M, McNicol J, Russell J, Collins T, Draper JS (2013) Lengthened G1 phase indicates differentiation status in human embryonic stem cells. *Stem Cells Dev* 22: 279 – 295

Chen T, Dent SY (2014) Chromatin modifiers and remodellers: regulators of cellular differentiation. *Nat Rev Genet* 15: 93 – 106

Cheng J, Blum R, Bowman C, Hu D, Shilatifard A, Shen S, Dynlacht BD (2014) A role for H3K4 monomethylation in gene repression and partitioning of chromatin readers. *Mol Cell* 53: 979 – 992

Coronado D, Godet M, Bourillot PY, Tapponnier Y, Bernat A, Petit M, Afanassieff M, Markossian S, Malashicheva A, Iacone R, Anastassiadis K, Savatier P (2013) A short G1 phase is an intrinsic determinant of naive embryonic stem cell pluripotency. *Stem Cell Res* 10: 118 – 131

Cowley SM, Iritani BM, Mendrysa SM, Xu T, Cheng PF, Yada J, Liggitt HD, Eisenman RN (2005) The mSin3A chromatin-modifying complex is essential for embryogenesis and T-cell development. *Mol Cell Biol* 25: 6990 – 7004

Cox J, Mann M (2008) MaxQuant enables high peptide identification rates, individualized p.p.b.-range mass accuracies and proteome-wide protein quantification. *Nat Biotechnol* 26: 1367 – 1372

Dannenberg JH, David G, Zhong S, van der Torre J, Wong WH, Depinho RA (2005) mSin3A corepressor regulates diverse transcriptional networks governing normal and neoplastic growth and survival. *Genes Dev* 19: 1581 – 1595

De Nadal E, Zapater M, Alepuz PM, Sumoy L, Mas G, Posas F (2004) The MAPK Hog1 recruits Rpd3 histone deacetylase to activate osmoresponsive genes. *Nature* 427: 370 – 374

Denissov S, Hofemeister H, Marks H, Kranz A, Ciotta G, Singh S, Anastassiadis K, Stunnenberg HG, Stewart AF (2014) Mll2 is required for H3K4 trimethylation on bivalent promoters in embryonic stem cells, whereas Mll1 is redundant. *Development* 141: 526 – 537

Di Giammartino DC, Apostolou E (2016) The chromatin signature of pluripotency: establishment and maintenance. *Curr Stem Cell Rep* 2: 255 – 262

Dobin A, Davis CA, Schlesinger F, Drenkow J, Zaleski C, Jha S, Batut P, Chaisson M, Gingeras TR (2013) STAR: ultrafast universal RNA-seq aligner. *Bioinformatics* 29: 15 – 21

Efroni S, Duttagupta R, Cheng J, Dehghani H, Hoeppner DJ, Dash C, Bazett-Jones DP, Le Grice S, McKay RD, Buetow KH, Gingeras TR, Misteli T, Meshorer E (2008) Global transcription in pluripotent embryonic stem cells. *Cell Stem Cell* 2: 437 – 447

Fleischer TC, Yun UJ, Ayer DE (2003) Identification and characterization of three new components of the mSin3A corepressor complex. *Mol Cell Biol* 23: 3456 – 3467

Grzenda A, Lomberk G, Zhang JS, Urrutia R (2009) Sin3: master scaffold and transcriptional corepressor. *Biochem Biophys Acta* 1789: 443 – 450

Hassig CA, Fleischer TC, Billin AN, Schreiber SL, Ayer DE (1997) Histone deacetylase activity is required for full transcriptional repression by mSin3A. *Cell* 89: 341 – 347

Ho L, Ronan JL, Wu J, Staahl BT, Chen L, Kuo A, Lessard J, Nesvizhskii AI, Ranish J, Crabtree GR (2009) An embryonic stem cell chromatin remodeling complex, esBAF, is essential for embryonic stem cell self-renewal and pluripotency. *Proc Natl Acad Sci USA* 106: 5181 – 5186

Ho L, Crabtree GR (2010) Chromatin remodelling during development. *Nature* 463: 474 – 484

Itoh F, Watabe T, Miyazono K (2014) Roles of TGF-beta family signals in the fate determination of pluripotent stem cells. *Semin Cell Dev Biol* 32: 98 – 106

Kareta MS, Sage J, Wernig M (2015) Crosstalk between stem cell and cell cycle machineries. *Curr Opin Cell Biol* 37: 68 – 74

Kelly RD, Cowley SM (2013) The physiological roles of histone deacetylase (HDAC) 1 and 2: complex co-stars with multiple leading parts. *Biochem Soc Trans* 41: 741 – 749

Kloet SL, Makowski MM, Baymaz HI, van Voorthuijsen L, Karemaker ID, Santanach A, Jansen PW, Di Croce L, Vermeulen M (2016) The dynamic interactome and genomic targets of Polycomb complexes during stem-cell differentiation. *Nat Struct Mol Biol* 23: 682 – 690

Kuzmichev A, Zhang Y, Erdjument-Bromage H, Tempst P, Reinberg D (2002) Role of the Sin3-histone deacetylase complex in growth regulation by the candidate tumor suppressor p33(ING1). *Mol Cell Biol* 22: 835 – 848

Laherty CD, Billin AN, Lavinsky RM, Yochum GS, Bush AC, Sun JM, Mullen TM, Davie JR, Rose DW, Glass CK, Rosenfeld MG, Ayer DE, Eisenman RN (1998) SAP30, a component of the mSin3 corepressor complex involved in N-CoR-mediated repression by specific transcription factors. *Mol Cell* 2: 33 – 42

Lai A, Kennedy BK, Barbie DA, Bertos NR, Yang XJ, Theberge MC, Tsai SC, Seto E, Zhang Y, Kuzmichev A, Lane WS, Reinberg D, Harlow E, Branton PE (2001) RBP1 recruits the mSIN3-histone deacetylase complex to the pocket of retinoblastoma tumor suppressor family proteins found in limited discrete regions of the nucleus at growth arrest. *Mol Cell Biol* 21: 2918 – 2932

Langmead B, Salzberg SL (2012) Fast gapped-read alignment with Bowtie 2. *Nat Methods* 9: 357 – 359

Lanigan F, Geraghty JG, Bracken AP (2011) Transcriptional regulation of cellular senescence. *Oncogene* 30: 2901 – 2911

Laugesen A, Helin K (2014) Chromatin repressive complexes in stem cells, development, and cancer. *Cell Stem Cell* 14: 735 – 751

Lee JH, Hart SR, Skalnik DG (2004) Histone deacetylase activity is required for embryonic stem cell differentiation. *Genesis* 38: 32 – 38

Lessard J, Wu JI, Ranish JA, Wan M, Winslow MM, Staahl BT, Wu H, Aebersold R, Graef IA, Crabtree GR (2007) An essential switch in subunit composition of a chromatin remodeling complex during neural development. *Neuron* 55: 201 – 215

Liang G, Zhang Y (2013) Embryonic stem cell and induced pluripotent stem cell: an epigenetic perspective. *Cell Res* 23: 49 – 69

Love MI, Huber W, Anders S (2014) Moderated estimation of fold change and dispersion for RNA-seq data with DESeq2. *Genome Biol* 15: 550

McDonel P, Costello I, Hendrich B (2009) Keeping things quiet: roles of NuRD and Sin3 co-repressor complexes during mammalian development. *Int J Biochem Cell Biol* 41: 108 – 116

McDonel P, Demmers J, Tan DW, Watt F, Hendrich BD (2012) Sin3a is essential for the genome integrity and viability of pluripotent cells. *Dev Biol* 363: 62 – 73

Meshorer E, Misteli T (2006) Chromatin in pluripotent embryonic stem cells and differentiation. *Nat Rev Mol Cell Biol* 7: 540 – 546

Meshorer E, Yellajoshula D, George E, Scambler PJ, Brown DT, Misteli T (2006) Hyperdynamic plasticity of chromatin proteins in pluripotent embryonic stem cells. *Dev Cell* 10: 105 – 116

Metivier R, Penot G, Hubner MR, Reid G, Brand H, Kos M, Gannon F (2003) Estrogen receptor-alpha directs ordered, cyclical, and combinatorial recruitment of cofactors on a natural target promoter. *Cell* 115: 751 – 763

Munoz IM, MacArtney T, Sanchez-Pulido L, Ponting CP, Rocha S, Rouse J (2012) Family with sequence similarity 60A (FAM60A) protein is a cell cycle-fluctuating regulator of the SIN3-HDAC1 histone deacetylase complex. *J Biol Chem* 287: 32346 – 32353

Nascimento EM, Cox CL, MacArthur S, Hussain S, Trotter M, Blanco S, Suraj M, Nichols J, Kubler B, Benitah SA, Hendrich B, Odom DT, Frye M (2011) The opposing transcriptional functions of Sin3a and c-Myc are required to maintain tissue homeostasis. *Nat Cell Biol* 13: 1395 – 1405

Nikolaev AY, Papanikolaou NA, Li M, Qin J, Gu W (2004) Identification of a novel BRMS1-homologue protein p40 as a component of the mSin3A/p33 (ING1b)/HDAC1 deacetylase complex. *Biochem Biophys Res Comm* 323: 1216 – 1222

van Nuland R, Smits AH, Pallaki P, Jansen PW, Vermeulen M, Timmers HT (2013) Quantitative dissection and stoichiometry determination of the human SET1/MLL histone methyltransferase complexes. *Mol Cell Biol* 33: 2067 – 2077

van Oevelen C, Bowman C, Pellegrino J, Asp P, Cheng J, Parisi F, Micsinai M, Kluger Y, Chu A, Blais A, David G, Dynlacht BD (2010) The mammalian Sin3 proteins are required for muscle development and sarcomere specification. *Mol Cell Biol* 30: 5686 – 5697

Oliviero G, Munawar N, Watson A, Streubel G, Manning G, Bardwell V, Bracken AP, Cagney G (2015) The variant polycomb repressor complex 1 component PCGF1 interacts with a pluripotency sub-network that includes DPPA4, a regulator of embryogenesis. *Sci Rep* 5: 18388

Oliviero G, Brien GL, Waston A, Streubel G, Jerman E, Andrews D, Doyle B, Munawar N, Wynne K, Crean J, Bracken AP, Cagney G (2016) Dynamic protein interactions of the polycomb repressive complex 2 during differentiation of pluripotent cells. *Mol Cell Proteomics* 15: 3450 – 3460

Park KS (2011) Tgf-Beta family signaling in embryonic stem cells. *Int J Stem Cells* 4: 18 – 23

Pasini D, Bracken AP, Hansen JB, Capillo M, Helin K (2007) The polycomb group protein Suz12 is required for embryonic stem cell differentiation. *Mol Cell Biol* 27: 3769 – 3779

Pellegrino J, Castrillon DH, David G (2012) Chromatin associated Sin3A is essential for male germ cell lineage in the mouse. *Dev Biol* 369: 349 – 355

Piunti A, Rossi A, Cerutti A, Albert M, Jammula S, Scelfo A, Cedrone L, Fragola G, Olsson L, Koseki H, Testa G, Casola S, Helin K, d'Adda di Fagagna F, Pasini D (2014) Polycomb proteins control proliferation and transformation independently of cell cycle checkpoints by regulating DNA replication. *Nat Commun* 5: 3649

Quinlan AR, Hall IM (2010) BEDTools: a flexible suite of utilities for comparing genomic features. *Bioinformatics* 26: 841 – 842

Reynolds N, O'Shaughnessy A, Hendrich B (2013) Transcriptional repressors: multifaceted regulators of gene expression. *Development* 140: 505 – 512

Riising EM, Comet I, Leblanc B, Wu X, Johansen JV, Helin K (2014) Gene silencing triggers polycomb repressive complex 2 recruitment to CpG islands genome wide. *Mol Cell* 55: 347 – 360

Ruijtenberg S, van den Heuvel S (2016) Coordinating cell proliferation and differentiation: antagonism between cell cycle regulators and cell type-specific gene expression. *Cell Cycle* 15: 196 – 212

Ruiz-Roig C, Vieitez C, Posas F, de Nadal E (2010) The Rpd3L HDAC complex is essential for the heat stress response in yeast. *Mol Microbiol* 76: 1049 – 1062

Sardiu ME, Smith KT, Groppe BD, Gilmore JM, Saraf A, Egidy R, Peak A, Seidel CW, Florens L, Workman JL, Washburn MP (2014) Suberoylanilide hydroxamic acid (SAHA)-induced dynamics of a human histone deacetylase protein interaction network. *Mol Cell Proteomics* 13: 3114 – 3125

Saunders A, Huang X, Fidalgo M, Reimer MH Jr, Faiola F, Ding J, Sanchez-Priego C, Guallar D, Saenz C, Li D, Wang J (2017) The SIN3A/HDAC corepressor complex functionally cooperates with NANOG to promote pluripotency. *Cell Rep* 18: 1713 – 1726

Schoenfelder S, Furlan-Magaril M, Mifsud B, Tavares-Cadete F, Sugar R, Javierre BM, Nagano T, Katsman Y, Sakthidevi M, Wingett SW, Dimitrova E, Dimond A, Edelman LB, Elderkin S, Tabbada K, Darbo E, Andrews S, Herman B, Higgs A, LeProust E *et al* (2015) The pluripotent regulatory circuitry connecting promoters to their long-range interacting elements. *Genome Res* 25: 582 – 597

Shen L, Shao N, Liu X, Nestler E (2014) ngs.plot: quick mining and visualization of next-generation sequencing data by integrating genomic databases. *BMC Genom* 15: 284

Shi X, Hong T, Walter KL, Ewalt M, Michishita E, Hung T, Carney D, Pena P, Lan F, Kaadige MR, Lacoste N, Cayrou C, Davrazou F, Saha A, Cairns BR, Ayer DE, Kutateladze TG, Shi Y, Cote J, Chua KF *et al* (2006) ING2 PHD domain links histone H3 lysine 4 methylation to active gene repression. *Nature* 442: 96 – 99

Silverstein RA, Ekwall K (2005) Sin3: a flexible regulator of global gene expression and genome stability. *Curr Genet* 47: 1 – 17

Skowyra D, Zeremski M, Neznanov N, Li M, Choi Y, Uesugi M, Hauser CA, Gu W, Gudkov AV, Qin J (2001) Differential association of products of alternative transcripts of the candidate tumor suppressor ING1 with the mSin3/HDAC1 transcriptional corepressor complex. *J Biol Chem* 276: 8734 – 8739

Smith KT, Martin-Brown SA, Florens L, Washburn MP, Workman JL (2010) Deacetylase inhibitors dissociate the histone-targeting ING2 subunit from the Sin3 complex. *Chem Biol* 17: 65 – 74

Smith KT, Sardiu ME, Martin-Brown SA, Seidel C, Mushegian A, Egidy R, Florens L, Washburn MP, Workman JL (2012) Human family with sequence similarity 60 member A (FAM60A) protein: a new subunit of the Sin3 deacetylase complex. *Mol Cell Proteomics* 11: 1815 – 1828

Smits AH, Jansen PW, Poser I, Hyman AA, Vermeulen M (2013) Stoichiometry of chromatin-associated protein complexes revealed by label-free quantitative mass spectrometry-based proteomics. *Nucleic Acids Res* 41: e28

Tyanova S, Temu T, Sinitcyn P, Carlson A, Hein MY, Geiger T, Mann M, Cox J (2016) The Perseus computational platform for comprehensive analysis of (prote)omics data. *Nat Methods* 13: 731 – 740

Vella P, Scelfo A, Jammula S, Chiacchiera F, Williams K, Cuomo A, Roberto A, Christensen J, Bonaldi T, Helin K, Pasini D (2013) Tet proteins connect the O-linked N-acetylglucosamine transferase Ogt to chromatin in embryonic stem cells. *Mol Cell* 49: 645 – 656

Vidal M, Strich R, Esposito RE, Gaber RF (1991) RPD1 (SIN3/UME4) is required for maximal activation and repression of diverse yeast genes. *Mol Cell Biol* 11: 6306 – 6316

Wang Z, Zang C, Cui K, Schones DE, Barski A, Peng W, Zhao K (2009) Genome-wide mapping of HATs and HDACs reveals distinct functions in active and inactive genes. *Cell* 138: 1019 – 1031

Williams K, Christensen J, Pedersen MT, Johansen JV, Cloos PA, Rappsilber J, Helin K (2011) TET1 and hydroxymethylcytosine in transcription and DNA methylation fidelity. *Nature* 473: 343 – 348

Wisniewski JR, Zougman A, Nagaraj N, Mann M (2009) Universal sample preparation method for proteome analysis. *Nat Methods* 6: 359 – 362

Wu H, D'Alessio AC, Ito S, Xia K, Wang Z, Cui K, Zhao K, Sun YE, Zhang Y (2011) Dual functions of Tet1 in transcriptional regulation in mouse embryonic stem cells. *Nature* 473: 389 – 393

Wu H, Zhang Y (2011) Tet1 and 5-hydroxymethylation: a genome-wide view in mouse embryonic stem cells. *Cell Cycle* 10: 2428 – 2436

Yamaji M, Ueda J, Hayashi K, Ohta H, Yabuta Y, Kurimoto K, Nakato R, Yamada Y, Shirahige K, Saitou M (2013) PRDM14 ensures naive pluripotency through dual regulation of signaling and epigenetic pathways in mouse embryonic stem cells. *Cell Stem Cell* 12: 368 – 382

Yang X, Zhang F, Kudlow JE (2002) Recruitment of O-GlcNAc transferase to promoters by corepressor mSin3A: coupling protein O-GlcNAcylation to transcriptional repression. *Cell* 110: 69 – 80

Yeo JC, Jiang J, Tan ZY, Yim GR, Ng JH, Goke J, Kraus P, Liang H, Gonzales KA, Chong HC, Tan CP, Lim YS, Tan NS, Lufkin T, Ng HH (2014) Klf2 is an essential factor that sustains ground state pluripotency. *Cell Stem Cell* 14: 864 – 872

Zhang Y, Iratni R, Erdjument-Bromage H, Tempst P, Reinberg D (1997) Histone deacetylases and SAP18, a novel polypeptide, are components of a human Sin3 complex. *Cell* 89: 357 – 364

Zhang Y, Sun ZW, Iratni R, Erdjument-Bromage H, Tempst P, Hampsey M, Reinberg D (1998) SAP30, a novel protein conserved between human and yeast, is a component of a histone deacetylase complex. *Mol Cell* 1: 1021 – 1031

Zhang Y, Liu T, Meyer CA, Eeckhoute J, Johnson DS, Bernstein BE, Nusbaum C, Myers RM, Brown M, Li W, Liu XS (2008) Model-based analysis of ChIP-Seq (MACS). *Genome Biol* 9: R137

